# The mitochondrial membrane protein FgLetm1 regulates mitochondrial integrity, production of endogenous reactive oxygen species and mycotoxin biosynthesis in Fusarium graminearum



| | |
|---|---|
| Journal: | *Molecular Plant Pathology* |
| Manuscript ID | MPP-OA-17-227.R2 |
| Manuscript Type: | Original Article |
| Date Submitted by the Author: | n/a |



| | |
|---|---|
| Complete List of Authors: | Tang, Guangfei; Institute of Biotechnology, Zhejiang University, 310058<br>Zhang, Chengqi; Institute of Biotechnology, Zhejiang University, 310058; College of Plant Protection, Anhui Agricultural University, 230036<br>Ju, Zhenzhen; Institute of Biotechnology, Zhejiang University, 310058<br>Zheng, Shiyu; Institute of Biotechnology, Zhejiang University, 310058<br>Wen, Ziyue; Institute of Biotechnology, Zhejiang University, 310058<br>Xu, Sunde; Institute of Biotechnology, Zhejiang University, 310058<br>Chen, Yun; Institute of Biotechnology, Zhejiang University, 310058<br>Ma, Zhonghua; Institute of Biotechnology, Zhejiang University, 310058 |



| | |
|---|---|
| Keywords: | Fusarium graminearum, Endogenous reactive oxygen species, FgLetm1, Mitochondrial integrity, Mycotoxin, Virulence |


SCHOLARONE™
Manuscripts

1 2 3 4 5 6 7 8 9 10 11 12 13 14 15 16 17 18 19 20 21 22 23 24 25 26 27 28 29 30 31 32 33 34 35 36 37 38 39 40 41 42 43 44 45 46 47 48 49 50 51 52 53 54 55 56 57 58 59 60

1 **The mitochondrial membrane protein FgLetm1 regulates mitochondrial**
2 **integrity, production of endogenous reactive oxygen species and**
3 **mycotoxin biosynthesis in *Fusarium graminearum***

4 Guangfei Tang[1†], Chengqi Zhang[1,2†], Zhenzhen Ju[1], Shiyu Zheng[1], Ziyue Wen[1],
5 Sunde Xu[1], Yun Chen[1*] and Zhonghua Ma[1]
6 [1] Institute of Biotechnology, Zhejiang University, Hangzhou, 310058, China
7 [2] College of Plant Protection, Anhui Agricultural University, Hefei 230036,
8 China
9 ***Corresponding author:**
10 Yun Chen
11 Email: chenyun0927@zju.edu.cn;
12 Tel. & Fax (+86) 571 88982106.
13 † These authors contributed equally to this work.

Proof

14

15 **RUNNING TITLE**:
16 Function of FgLetm1 in *Fusarium graminearum*

17 **KEYWORDS**:
18 *Fusarium graminearum*; Endogenous reactive oxygen species; FgLetm1;
19 Mitochondrial integrity; Mycotoxin; Virulence.
20 Word count: 6997; Figure number: 8; Table number: 3.

SUMMARY

Deoxynivalenol (DON) is a mycotoxin produced in cereal crops infected with *Fusarium graminearum*. DON poses a serious threat to human and animal health and is a critical virulence factor. Various environmental factors including reactive oxygen species (ROS) have been shown to interfere with DON biosynthesis in this pathogen. The regulatory mechanisms of how ROS trigger DON production have been extensively investigated in *F. graminearum*. However, the role of the endogenous ROS generating system in DON biosynthesis is largely unknown. In this study, we genetically analyzed the function of Leucine zipper–EF-hand–containing trans-membrane 1(LETM1) super-family proteins and evaluated the role of the mitochondria-produced ROS in DON biosynthesis. Our results show that there are two Letm1 orthologs, FgLetm1 and FgLetm2, in *F. graminearum*. FgLetm1 is localized to the mitochondria and is essential for mitochondrial integrity, whereas FgLetm2 plays a minor role in maintaining mitochondrial integrity. The ΔFgLetm1 mutant demonstrated a vegetative growth defect, abnormal conidia and increased sensitivity to various stress agents. More importantly, the ΔFgLetm1 mutant showed significantly reduced levels of endogenous ROS, decreased DON biosynthesis and attenuated virulence *in planta*. To our knowledge, this is the first report that mitochondrial integrity and endogenous ROS production by mitochondria are important for DON production and virulence in *Fusarium* species.

Proof

1
2
3 43 **INTRODUCTION**
4
5 44 Deoxynivalenol (DON) is the most prevalent and economically important
6
7 45 mycotoxin associated with infested grains by *Fusarium* species (Desjardins,
8
9 46 2006). Among the *Fusarium* fungi, *Fusarium graminearum* is the main DON
10
11 47 producer that causes a devastating disease known as Fusarium Head Blight
12
13 48 (FHB) in cereal crops worldwide (Bennett & Klich, 2003, Desjardins, 2006,
14
15 49 Kimura *et al.*, 2007). The biosynthetic pathway of DON has been extensively
16
17 50 studied, and nearly all genes involved in DON biosynthesis (*TRI* genes) have
18
19 51 been identified (Desjardins *et al.*, 1993, Kimura *et al.*, 2001, Kimura et al.,
20
21 52 2007). Biosynthesis of secondary metabolites including mycotoxins is
22
23 53 influenced by various environmental factors. Previous investigations on the
24
25 54 regulation of DON biosynthesis in *F. graminearum* revealed the influence of
26
27 55 mycotoxin production by environmental or extra-cellular factors, such as
28
29 56 nitrogen and carbon sources (Jiao *et al.*, 2008, Miller & Greenhalgh, 1985, Oh
30
31 57 *et al.*, 2016), pH (Merhej *et al.*, 2011), magnesium (Pinson-Gadais *et al.*, 2009),
32
33 58 phenolic acids (Boutigny *et al.*, 2009), and amines (Gardiner *et al.*, 2009). Our
34
35 59 recent study showed that methylation of histone H3K4 also contributed to DON
36
37 60 production (Liu *et al.*, 2015). In addition to those factors, reactive oxygen
38
39 61 species (ROS) have been highlighted as a stimulator interfering with DON
40
41 62 production (Audenaert *et al.*, 2010, Ponts *et al.*, 2007, Ponts *et al.*, 2006,
42
43 63 Montibus *et al.*, 2013, Jiang *et al.*, 2015). Supplementation with hydrogen
44
45 64 peroxide ($H_2O_2$) or the fungicide prothioconazole to the liquid cultures of *F.*
46
47 65 *graminearum* were able to significantly increase the concentration of
48
49 66 intracellular ROS, which subsequently stimulated *TRI* gene expression and
50
51 67 induced DON production (Audenaert *et al.*, 2010, Ponts *et al.*, 2007, Ponts *et*
52
53
54
55
56
57
58
59
60

Proof

1
2
3 68 *al.*, 2006). Relatively higher concentrations of $H_2O_2$ were observed in the
4
5 69 infection cushions, as compared to runner hyphae during the infection process
6
7 70 of *F. graminearum* (Mentages & Bormann, 2015). However, the mechanism to
8
9 71 generate endogenous ROS, and the role of ROS the regulation of DON
10
11 72 biosynthesis remain relatively unknown in *F. graminearum*.

73 ROS are able to cause DNA damage, lipid peroxidation, and protein oxidation (Beckman & Ames, 1998). Alternatively, ROS have been suggested to be a secondary messenger that transduces signals to regulate cellular functions such as immunity, cell proliferation and ion transport in mammals and plants. In microbial eukaryotes, ROS have been shown to be involved in regulation of life-span (Osiewacz, 2002), host-pathogen interactions and other cellular functions (Missall *et al.*, 2004, Nowikovsky *et al.*, 2004). Mitochondria are the major source of endogenous ROS, and produce about 95% of the total of ROS during cellular oxidative metabolism (Liu, 1999). Meanwhile, several enzymatic and non-enzymatic systems are also involved in intracellular ROS production (Grissa *et al.*, 2010). The most important enzymatic ROS-generating system is the NADPH-dependent oxidase complex (Nox). The role of NADPH oxidases NoxA and NoxB and the regulator NoxR in ROS production have been investigated in *F. graminearum* (Wang *et al.*, 2014, Zhang *et al.*, 2016). However, the roles of mitochondria and the mitochondrial ROS-generating system in secondary metabolism and virulence of phytopathogenic fungi, including *F. graminearum,* have not been investigated.

**L**eucine zipper–**E**F-hand–containing **t**rans**m**embrane 1(LETM1), an inner mitochondrial membrane protein, has been identified as a protein associated with Wolf-Hirschhorn syndrome (WHS), a complex multigenic human disease

Proof

1
2
3
4
5
6
7
8
9
10
11
12
13
14
15
16
17
18
19
20
21
22
23
24
25
26
27
28
29
30
31
32
33
34
35
36
37
38
39
40
41
42
43
44
45
46
47
48
49
50
51
52
53
54
55
56
57
58
59
60

93 caused by the partial deletion of the distal short arm of chromosome 4 (Endele
94 *et al.*, 1999, Zollino *et al.*, 2003). Letm1 is evolutionarily conserved from yeast
95 to mammals. The biological functions of the Letm1 orthologs have been
96 investigated in various organisms (Dimmer *et al.*, 2008, Hasegawa & van der
97 Bliek, 2007, Hashimi *et al.*, 2013, McQuibban *et al.*, 2010, Nowikovsky et al.,
98 2004, Zhang *et al.*, 2012). However, the function of the Letm1 super-family in
99 filamentous fungi is still largely unknown. In this study, the Letm1 orthologs
100 were selected as target proteins to investigate the biological function of ROS
101 generated from mitochondria and mitochondrial integrity in DON biosynthesis,
102 virulence and cell development. Our results showed that the deletion mutant
103 ΔFgLetm1 had a vegetative growth defect and abnormal conidia. The mutant
104 was also more sensitive to various stress agents. More importantly, ΔFgLetm1
105 significantly reduced the levels of cellular ROS, decreased DON biosynthesis
106 and attenuated virulence *in planta*.

Proof

107

108 **RESULTS**

109 **Identification and sequence analysis of Letm1-like proteins in *Fusarium***
110 ***graminearum***

111 A BLASTP search using *Saccharomyces cerevisiae* Letm1 family proteins,
112 Mdm38 and Ylh47, as queries in the *F. graminearum* genome revealed only
113 one putative Letm1 gene in this fungus, FGSG_09158 (designated as
114 FgLetm1). The *FgLETM1* gene is predicted to encode a protein with 550
115 amino acids, sharing 47% and 45% sequence identity with Mdm38 and Ylh47,
116 respectively. Meanwhile, we retrieved other genes with the LETM1
117 super-family domain in the *F. graminearum* genome, and found that the

1
2
3 118 FGSG_10063 locus (designated as FgLetm2) also contained a LETM1
4
5 119 super-family domain. However, FgLetm2 shares very low sequence identity
6
7 120 with Mdm38 and Ylh47 (9.8% and 11.4%, respectively). Similar to *S.*
8
9 121 *cerevisiae* Letm1 orthologs, FgLetm1 contains a noncanonical Letm1 protein
10
11 122 structure with a Letm1 super-family domain, a transmembrane (TM) domain
12
13 123 and a coiled-coil domain at the carboxyl terminus. The FgLetm2 protein
14
15 124 harbors a truncated Letm1 super-family domain after the TM domain at the
16
17 125 carboxyl terminus (Fig. 1a). Both FgLetm1 and FgLetm2 lack the EF-hand
18
19 126 domain present in human Letm1 (NP_036450). This was consistent with a
20
21 127 previous study, in which it was demonstrated that the EF-hand domain was
22
23 128 absent in lower eukaryotes, fungi and plasmodium (Nowikovsky et al., 2004).
24
25 129 To gain more insight into the Letm1 evolution in fungi, we retrieved all
26
27 130 genes that encode proteins containing the Letm1 super-family domain from 32
28
29 131 fungal genomes available in the NCBI Bioprojects and Broad Institute
30
31 132 database. The results indicated that genes for the Letm1-like proteins are
32
33 133 highly conserved in fungi, while the number of orthologs varies in different
34
35 134 fungal species. Most fungal species (25 out 32) harbored two orthologs, albeit
36
37 135 the representative fungi from *Taphrinomycotina*, *Pucciniomycotina* and
38
39 136 *Chytridiomycota* contained only one Letm1-like protein. Moreover, three
40
41 137 different genes encoding the Letm1-like proteins were retrieved from
42
43 138 *Zygomycota* fungi *Rhizopus oryzae* and *Mucor circinelloides* (Fig. S1). A
44
45 139 phylogenetic analysis of the putative Letm1-like proteins, which include *F.*
46
47 140 *graminearum* and six filamentous phytopathogenic fungi, showed that the
48
49 141 Letm1-like proteins are significantly divided into two groups (Fig. 1b). Proteins
50
51 142 in group II had a truncated Letm1 super-family domain with a length of 58-75
52
53
54
55
56
57
58
59
60

Proof

1
2
3 143 amino acids (Table S1). The domain characteristic and the phylogenetic tree
4
5 144 indicated that FgLetm1 might have similar biological functions to the Letm1
6
7 145 proteins Mdm38 and Yln47 in *S. cerevisiae*.
8
9 146 In addition, our in-house RNA-seq data indicated that the transcriptional
10
11 147 level of *FgLETM1* was higher than that of *FgLETM2*, by a range of 5- to 20-
12
13 148 fold higher, in all four tested conditions including in the conidiation medium
14
15 149 (CMC), hyphae grown in PDA, plant infection and deoxynivalenol (DON)
16
17 150 biosynthesis induction medium (TBI) (Fig. 1c).
18
19 151 **Disruption of FgLetm1 and FgLetm2**
20
21 152 To characterize the function of FgLetm1 and FgLetm2, we generated single
22
23 153 and double deletion mutants, ΔFgLetm1, ΔFgLetm2 and ΔΔFgLetm1/2, using
24
25 154 the homologous recombination strategy. The single or double deletion mutants
26
27 155 were confirmed by Southern hybridization assays (Fig. S2). To confirm that the
28
29 156 phenotypic abnormalities of the mutants were directly related to the deletion,
30
31 157 we complemented the deletion mutants with the gene fused with *gfp* for the
32
33 158 green florescent protein (GFP) at the carboxyl terminus under their native
34
35 159 promoters, respectively, and generated the complemented strain ΔFgLetm1-C
36
37 160 (ΔFgLetm1+$P_{LETM1}$ FgLetm1-GFP) and ΔFgLetm2-C (ΔFgLetm2+$P_{LETM2}$
38
39 161 FgLetm2-GFP) . The complemented strains were also confirmed by Southern
40
41 162 blot assays and PCR amplification (Fig. S2).
42
43 163 **FgLetm1 regulates hyphal growth, conidiation and conidial germination**
44
45 164 The ΔFgLetm1 mutant demonstrated radial and hyphal growth defects. The
46
47 165 rate of radial growth of ΔFgLetm1 was reduced on both PDA (potato dextrose
48
49 166 agar) and MM (minimal medium), in comparison with that of wild type PH-1,
50
51 167 respectively. Moreover, the deletion mutant of ΔFgLetm1 exhibited a reduction
52
53
54
55
56
57
58
59
60



Proof

1
2
3
4
5
6
7
8
9
10
11
12
13
14
15
16
17
18
19
20
21
22
23
24
25
26
27
28
29
30
31
32
33
34
35
36
37
38
39
40
41
42
43
44
45
46
47
48
49
50
51
52
53
54
55
56
57
58
59
60

168 in aerial hyphae formation on solid agar plates (Fig. 2 a).

169 ΔFgLetm1 produced less conidia than that of the wild type PH-1 after 4
170 days of incubation in CMC (Table 1). To further examine conidial morphology,
171 calcofluor white staining assays were performed for individual mutants. The
172 results were observed under the fluorescent microscope. As shown in Fig. S3
173 and Table 1, the size of conidia produced by ΔFgLetm1 was shorter, in
174 comparison with that of the wild type. Moreover, the conidia of ΔFgLetm1
175 harbored fewer septa. Most of the conidia (65%) had only 3 septa in the
176 ΔFgLetm1, while the majority of conidia produced by wild type had 5 septa (Fig.
177 2b). Meanwhile, the abnormal conidia of ΔFgLetm1 showed slower
178 germination than that of the wild type in the present of 2% sucrose (Fig. 2c).

179 In contrast, the deletion mutant of ΔFgLetm2 did not show visible
180 phenotypic differences in vegetative growth, conidia formation and germination,
181 in comparison with that of the wild type. The ΔΔFgLetm1/2 double mutant
182 demonstrated similar phenotypes as those in the ΔFgLetm1 single mutant.
183 Phenotypic defects of ΔFgLetm1 were restored by the complementation in the
184 complemented strain ΔFgLetm1-C (Fig. 2). Thus, our evidences confirmed that
185 the defects in the mutants were linked to the loss of the *FgLETM1* gene. Taken
186 together, the data presented here suggested that FgLetm1 is involved in the
187 hyphal growth, conidiation and conidial germination, and that FgLetm2 playes
188 a dispensable role in these biological processes under the tested conditions.

189 **Deletion mutant of ΔFgLetm1 showed increased sensitivity towards**
190 **osmotic stress, heat shock and fungicides**

191 It has been reported that Mdm38 is involved in resistance to several biotic
192 stresses in yeast (Frazier *et al.*, 2006, Sinha *et al.*, 2008, Dimmer *et al.*, 2002a).

Proof

1
2
3 193 Therefore, we were interested in determining the susceptibility of the mutants
4
5 194 in *F. graminearum* to various stresses, including osmotic stress, heat shock,
6
7 195 and fungicide treatment. The susceptibility assays showed that the ΔFgLetm1
8
9 196 mutant had a significantly increased sensitivity to osmotic stresses generated
10
11 197 by NaCl or KCl, whereas the ΔFgLetm2 mutant displayed the same
12
13 198 susceptibility to that of the wild type towards osmotic stresses (Figs. 3a, b).
14
15 199 The heat tolerance of the mutants was examined at 15 °C, 25 °C and 32 °C. As
16
17 200 shown in Fig. 3c, all strains displayed similar growth rate as that of the wild
18
19 201 type at 15 °C. For growth at 32 °C, noticeably, the ΔFgLetm1 mutant could not
20
21 202 grow at 32 °C. The complemented strains had similar growth rate and colony
22
23 203 morphology with the wild type PH-1. Therefore, our results indicated that
24
25 204 ΔFgLetm1 increased sensitivity to heat shock stress. To further confirm the
26
27 205 increase of sensitivity to high temperatures in ΔFgLetm1, we assayed the
28
29 206 transcriptional levels of the *FgHSP30* (Fg01158), *FgHSP70* (Fg00838), and
30
31 207 *FgGSY2*(Fg06822) genes, whose products are involved in the heat shock
32
33 208 tolerance in *F. graminearum* (Hu et al., 2014). When cultures were shifted from
34
35 209 25°C to 32°C for 1 h, the relative expression levels of *FgHSP70* and *FgHSP30*
36
37 210 were 2.5- and 2-fold higher, respectively, in PH-1 compared to that of
38
39 211 ΔFgLetm1 (Fig. 3d). Therefore, the deletion mutant of ΔFgLetm1 decreased
40
41 212 the expression of the selected heat stress response genes in *F. graminearum*.
42
43 213 The susceptibility of the mutants towards ions and fungicides were also
44
45 214 examined. ΔFgLetm1 displayed more sensitivity to iprodione, phenamacril,
46
47 215 $FeSO_4$ and $CaCl_2$ than that of the wild type and complemented strains (Fig. 3e,
48
49 216 f). In particular, the ΔFgLetm1 mutant was hyper-sensitive to $Fe^{2+}$ and could
50
51 217 not grow on the MM amended with 10 mM $Fe^{2+}$. It implied that FgLetm1 might
52
53
54
55
56
57
58
59
60

Proof

1
2
3 218 regulate the ferrum homeostasis in this fungus. The double mutant
4
5 219 ΔΔFgLetm1/2 showed similar phenotypes with that of ΔFgLetm1 in all tested
6
7 220 conditions.
8
9 221 **FgLetm1 is localized to the mitochondria and is critical for mitochondrial**
10
11 222 **integrity**
12
13 223 The complemented strains ΔFgLetm1-C and ΔFgLetm2-C with GFP-fusion
14
15 224 proteins were rescued for the phenotypice defects seen in the mutants (Figs.
16
17 225 2-3), indicating that the fusion proteins were functional. These strains were
18
19 226 further used for observing the subcellular localization of FgLetm1 and FgLetm2.
20
21 227 A filamentous network pattern of GFP signals was present in the vegetative
22
23 228 mycelia of the ΔFgLetm1-C strain (Fig. 4a). Co-localization experiments were
24
25 229 performed using dual-labeling with FgLetm1-GFP and mitochondrial indicator
26
27 230 Mito-HcRed staining. As shown in Fig. 4a, the GFP and Mito-HcRed signals
28
29 231 clearly overlapped, suggesting that FgLetm1 was localized to the mitochondria.
30
31 232 Using the same assay, we observated that FgLetm2-GFP was also
32
33 233 co-localized with Mito-HcRed (Fig. 4a). Therefore, both FgLetm1 and FgLetm2
34
35 234 were localized to the mitochondria.
36
37 235 Since both FgLetm1 and FgLemt2 were shown to be mitochondria
38
39 236 localized proteins, we were interested in testing whether the deletion mutants
40
41 237 would show altered mitochondrial structures. First, the mitochondrial patterns
42
43 238 were observed by Mito-HcRed staining. Mito-HcRed signal in the mycelia of
44
45 239 PH-1 and the complemented strains dominantly showed the filamentous
46
47 240 network shapes (Fig. 4b, video S1), while it displayed punctate patterns in the
48
49 241 mycelia of the ΔFgLetm1 single and the double mutant (Fig. 4b, video S2).
50
51 242 Interestingly, mitochodrial mobility was relatively slower in the ΔFgLetm1
52
53
54
55
56
57
58
59
60

Proof

1
2
3 243 mutant than in the wild type (videos S1, S2). This implied that the
4
5 244 mitochondrial morphology and function might be different in PH-1 and
6
7 245 ΔFgLetm1. Next, transmission electron microscope (TEM) experiment was
8
9 246 applied to visualize the details of the mitochondrial structures. The TEM
10
11 247 micrographs revealed that the deletion of the *FgLETM1* gene caused
12
13 248 mitochondrial swelling, an increase in mitochondrial volume and a lack of
14
15 249 tubular shaped cristae structures (Fig. 4c). The mitochondrial morphologies in
16
17 250 the ΔFgLetm2 cells showed similar shape and cristae structures in comparison
18
19 251 with that in PH-1, while the volume was slightly increased. The abnormal
20
21 252 mitochondrial morphologies of the double mutant were consistent with those of
22
23 253 the ΔFgLetm1 mutant (Figs. 4b, c).In yeast, Mdm38 is essential for the
24
25 254 biosynthesis of the respiratory chain components (Frazier et al., 2006). To test
26
27 255 whether FgLetm1 has a similar function in *F. graminearum*, we selected
28
29 256 cytochrome *b* (Cyt *b*) as the indicator protein of respiratory chain components,
30
31 257 and detected the protein level of Cytb by western blotting. As shown in Fig. 4d,
32
33 258 the abundance of the Cyt *b* protein was clearly decreased in ΔFgLetm1 and
34
35 259 the double mutant. Our findings thus strongly suggested that FgLetm1 is a
36
37 260 structural protein, which helps to maintain the mitochondrial structure and is
38
39 261 essential for the biosynthesis or the stability of the components in the
40
41 262 respiratory chain, whereas FgLetm2 might play a minor role in these
42
43 263 processes.
44
45 264 **The deletion mutant of ΔFgLetm1 decreased the production of**
46
47 265 **endogenous ROS and reduced ATP biosynthesis**
48
49 266 Mitochondria are an important source of ATP synthesis and ROS production in
50
51 267 eukaryotic cells. Given that the deletion mutant of ΔFgLetm1 resulted in
52
53
54
55
56
57
58
59
60



Proof

1
2
3 268 mitochondrial dysfunction, we next compared the concentration of intracellular
4
5 269 ROS and ATP biosynthesis in all above strains. The ROS content was
6
7 270 qualitatively analyzed with H2DCFDA (2', 7'-dichlorodihydrofluorescein
8
9
10 271 diacetate) staining in MM and TBI. As indicated in Fig. 5a, the mycelia of the
11
12 272 wild type, ΔFgLetm2 and complemented strains were all stained by the dye
13
14 273 and cells showed green signals under fluorescent microscope. Interestingly,
15
16 274 mycelia of the wild type, ΔFgLetm2 and complemented strains were swelled
17
18 275 and formed ovoid toxigenic cells, and displayed noticeably stronger green
19
20
21 276 signals in TBI (Fig. 5a, bottom panel) than in MM (Fig. 5a, upper panel). These
22
23 277 results suggested that ROS production were highly induced and ROS was
24
25 278 accumulated in cells during DON biosynthesis. However, limited fluorescent
26
27 279 signals were detected in ΔFgLetm1 and the double mutant in both media (Fig.
28
29
30 280 5a). Quantification data also confirmed that endogenous ROS was significantly
31
32 281 reduced in ΔFgLetm1 and ΔΔFgLetm1/2 (Table 2). Intracellular ROS levels
33
34 282 are usually balanced by the activities of catalases and superoxide dismutases.
35
36
37 283 Therefore, we performed qRT-PCR to measure the transcripts of seven
38
39 284 putative catalase and superoxide dismutase genes in the mycelia of the wild
40
41 285 type and the ΔFgLetm1 mutant after 3 days of incubation in TBI. As expected,
42
43 286 the qRT-PCR results indicated that all selected genes, except for *FgZnSOD2*,
44
45
46 287 showed very low transcriptional levels in ΔFgLetm1 in response to limited
47
48 288 intracellular ROS-mediated oxidative stress, in comparison with their
49
50 289 expression levels in the wild type (Fig. 5b). To determine whether the reduction
51
52 290 of intercellular ROS in ΔFgLetm1 and the double mutant would lead to their
53
54
55 291 higher tolerance towards extracellular ROS stress, we measured the sensitivity
56
57 292 of all strains to oxidative stress on the MM supplemented with 10 mM $H_2O_2$.
58
59
60

Proof

1 2 3 4 5 6 7 8 9 10 11 12 13 14 15 16 17 18 19 20 21 22 23 24 25 26 27 28 29 30 31 32 33 34 35 36 37 38 39 40 41 42 43 44 45 46 47 48 49 50 51 52 53 54 55 56 57 58 59 60

293 Deletion mutant of ΔFgLetm1 and the double mutant exhibited significantly
294 increased tolerance to oxidative stress mediated by $H_2O_2$ compared to that of
295 the wild type, ΔFgLetm2 and complemented strains (Fig. 5c, d).

296 We next measured ATP production in the deletion mutants. The
297 quantification data indicated that the production of ATP in the ΔFgLetm1 and
298 the double mutant was decreased about 30%, compared with that of the wild
299 type. The ΔFgLetm2 mutant and the complemented strains produced ATP at a
300 level similar to that of the wild type strain (Table 2). In mammals, LETM1
301 knock-down led to mitochondrial malfunction and an induction of glycolysis in
302 the cytoplasm to maintain their ATP supply in these cells (Dimmer et al., 2008,
303 Hwang *et al.*, 2010). To investigate whether the dysfunctional mitochondria in
304 ΔFgLetm1 also increases glycolysis, we measured the concentration of
305 ethanol, the byproduct of anaerobic respiration in fungi, in MM after 16 h of
306 incubation. As expected, the ethanol concentration of the cell-free supernatant
307 from the ΔFgLetm1 mutant was significantly elevated compared to the wild
308 type (Table 2), indicating that the *FgLETM1* deletion disrupted the respiration
309 chain and up-regulated the glycolytic pathway in *F. graminearum*. Collectively,
310 our data suggested that FgLetm1 is critical for normal mitochondrial function in
311 ATP generation and ROS production.

Proof

312 **The ΔFgLetm1 mutant is significantly attenuated in virulence**

313 On wheat heads inoculated with PH-1, or ΔFgLetm2, or the complemented
314 strains, scab symptoms were first developed on the inoculated spikelets and
315 rapidly spread to the whole wheat head after 15 days of inoculation. In contrast,
316 the hyphal growth of ΔFgLetm1 or the ΔΔFgLetm1/2 double mutant failed to
317 spread from the inoculated floret to the rachis, and subsequently caused scab

1
2
3
4
5
6
7
8
9
10
11
12
13
14
15
16
17
18
19
20
21
22
23
24
25
26
27
28
29
30
31
32
33
34
35
36
37
38
39
40
41
42
43
44
45
46
47
48
49
50
51
52
53
54
55
56
57
58
59
60

318 symptoms only in the inoculated spikelet (Fig. 6a, upper panel). Moreover,
319 almost all grains in infected wheat ears by wild-type PH-1, ΔFgLetm2 and
320 complemented strains were shriveled and bleached, while only the grain at the
321 inoculated site was shrunken in the treatment of ΔFgLetm1 and ΔΔFgLetm1/2
322 (Fig. 6a, bottom panel). Since that ΔFgLetm1 and ΔΔFgLetm1/2 mutants grew
323 well on the wheat head tissue medium (WA) (Fig. S4), the attenuated virulence
324 of ΔFgLetm1 and ΔΔFgLetm1/2 was not likely due to the growth defect. Next,
325 we investigated whether the deletion mutations affected the penetration
326 process. We examined the infection structures of strains during the infection
327 using scan electron microscope (SEM). Ultrastructural examination showed
328 that the hyphae of the wild type formed typical infection cushions on the
329 glumes at 48 h post-inoculation with conidia, but such penetration structures
330 were not observed on the glumes inoculated with conidia of either ΔFgLetm1
331 or ΔΔFgLetm1/2 under the same conditions. Both ΔFgLetm2 and the two
332 complemented strains showed similar infection structures on plant tissues to
333 those of the wild type (Fig. 6b). Noticeably, the ΔFgLetm1 mutant was capable
334 of penetrating the spikelet and resulted in the scab symptom after 2 weeks at
335 the inoculated sites (Figs. 6a, S5). These results suggested that the ΔFgLetm1
336 mutant delayed the penetration structure formation and was defective in
337 spreading from the inoculation site to nearby spikelets *via* the rachis. We
338 conclude that FgLetm1 is important in virulence in *F. graminearum*.

339 **FgLetm1 plays a critical role in DON biosynthesis**

340 DON biosynthesis in the mutants was evaluated both *in vitro* and *in planta*.
341 First, the transcriptional levels of *TRI* genes in the mutants were assayed by
342 qRT-PCR in TBI. All selected *TRI* genes were strongly down-regulated in the

Proof

1
2
3 343 ΔFgLetm1mutant, but the expression was not affected in ΔFgLetm2,
4
5 344 compared to those in the wild type (Fig. 7a). Next, the toxisome formation
6
7 345 (Boenisch *et al.*, 2017) for DON biosynthesis in the wild type and the mutants
8
9 346 was observed using the Tri1-GFP as an indicator in TBI cultures. As shown in
10
11 347 Fig. 7b, the Tri1-GFP was highly induced and formed spherical and crescent
12
13 348 toxisomes in the mycelia of the wild type and the ΔFgLetm2 mutant after 3
14
15 349 days of incubation in TBI. However, no visible green fluorescent signals were
16
17 350 observed in the mycelia of ΔFgLetm1 under the same condition. Consistent
18
19 351 with the expression of *TRI* genes and toxisomes formation, the amount of the
20
21 352 final product of DON biosynthesis in ΔFgLetm1 was strongly reduced by
22
23 353 18-fold when compared tp that in in the wild type in the TBI liquid medium
24
25 354 (Table 3). DON production was also significantly reduced in the ΔFgLetm1
26
27 355 deletion mutant in wheat grain cultures and the infested wheat kernels *in*
28
29 356 *planta*. The complemented strain ΔFgLetm1-C was completely restored in
30
31 357 DON production (Table 3). Collectively, our results suggest that FgLetm1 is
32
33 358 important in *TRI* gene expression and DON production in *F. graminearum*.
34
35 359 To determine whether the DON reduction is caused by decreased ATP and
36
37 360 ROS production in ΔFgLetm1, we conducted DON rescue assays by supplying
38
39 361 exogenous ATP or $H_2O_2$ in the liquid cultures induced by ammonium as
40
41 362 described previously (Gardiner et al., 2009). Treatment with $H_2O_2$ clearly
42
43 363 increased DON biosynthesis in PH-1, and partially recovered DON
44
45 364 biosynthesis in ΔFgLetm1(Fig. 7c). However, the final production of DON after
46
47 365 induction by $H_2O_2$ was still less than in the wild type (Fig. 7c). We next assayed
48
49 366 the expression of *TRI5*, *TRI6* and *TRI10* with RNA samples isolated from
50
51 367 hyphae of the wild-type and ΔFgLetm1 mutant with or without treatment of 0.5
52
53
54
55
56
57
58
59
60

Proof

1
2
3 368 mM $H_2O_2$ in LTB at day 3. In the wild type strain, the expression levels of *TRI5,*
4
5 369 *TRI6* and *TRI10* were 4.0-, 10.4- and 5.2-fold higher in $H_2O_2$-treated samples
6
7 370 than in untreated samples (Fig. 7d). Treatment with $H_2O_2$ also induced the
8
9 371 expression of these *TRI* genes in the ΔFgLetm1 mutant (Fig. 7d). However,
10
11 372 addition of exogenous ATP in TBI was unable to rescue the decreased of DON
12
13 373 biosynthesis in the ΔFgLetm1 mutant (Fig. S6). Therefore, our evidence
14
15 374 implied that the diminished endogenous ROS might be partly responsible for
16
17 375 the reduction of DON biosynthesis in ΔFgLetm1.
18
19 376 **Wild type *F. graminearum* produced less DON and was strongly**
20
21 377 **attenuated in virulence under the hypoxic condition.**
22
23 378 Given that dysfunctional mitochondria in the ΔFgLetm1 mutant increased the
24
25 379 activity of glycolysis, but decreased the DON biosynthesis and virulence, we
26
27 380 speculated that DON biosynthesis might be suppressed under hypoxic
28
29 381 condition. Therefore, we investigated DON biosynthesis and virulence of *F.*
30
31 382 *graminearum* under the limited $O_2$ condition (1%). Surprisingly, the radial
32
33 383 growth rate of the wild type PH-1 under hypoxic condition was similar to that
34
35 384 under the open air condition (Fig. 8a). Compared with the expression of *TRI5*,
36
37 385 *TRI6* and *TRI10* in TBI under the open air condition, the expression of these
38
39 386 genes in the wild type was strongly reduced under the hypoxic condition (Fig.
40
41 387 8b), which was similar levels to these in ΔFgLetm1 mutant (Fig. 7a). However,
42
43 388 the transcriptional level of the control gene *AURJ* for pigment formation was
44
45 389 increased under the hypoxic condition, indicating that the reduction of the *TRI*
46
47 390 gene expression was somehow specific under the hypoxic condition.
48
49 391 Meanwhile, the Tri1-GFP labeled toxisome formation was also completely
50
51 392 abolished under the hypoxic condition (Fig. 8c). Finally, the DON production
52
53
54
55
56
57
58
59
60



Proof

1
2
3 393 under hypoxic condition decreased by 40-fold than that in the open air (Fig. 8d).
4
5 394 The pathogenicity assay was also conducted under both conditions. After 7
6
7 395 days post-inoculation, the mycelia were able to infect the inoculated site,
8
9 396 caused the necrotic symptom, and spread to nearby spikelets under the open
10
11 397 air condition (Fig. 8e, left-hand panel). Remarkably, wild type PH-1 failed to
12
13 398 infect the inoculate spikelet under the hypoxia condition (Fig. 8e, right-hand
14
15 399 panel). Taken together, DON biosynthesis and virulence were suppressed in *F.*
16
17 400 *graminearum* under the low oxygen conditions, similar to the effect of
18
19 401 dysfunctional mitochondria caused by deletion of the *FgLETM1* gene.
20
21 402 **DISCUSSION**
22
23 403 Mdm38 in yeast is critical for the maintenance of mitochondrial morphology.
24
25 404 The lack or RNAi silencing of Letm1 orthologs led to the disruption of the
26
27 405 mitochondrial network and apparent swelling of the mitochondria in various
28
29 406 organisms (Dimmer *et al.*, 2002b, Nowikovsky et al., 2004, Schlickum *et al.*,
30
31 407 2004, Sickmann *et al.*, 2003, Hasegawa & van der Bliek, 2007, McQuibban et
32
33 408 al., 2010, Hashimi et al., 2013). To date, no study has been conducted to
34
35 409 investigate the biological roles of the Letm1 orthologs in filamentous fungi. In
36
37 410 this study, we showed that the ΔFgLetm1 mutant of the filamentous fungus *F.*
38
39 411 *graminearum* lacked tubular-shaped cristae structures and had increased
40
41 412 mitochondrial volumes (Fig. 4b-c). Interestingly, for the first time, we also
42
43 413 showed that FgLetm1 plays an important role in mitochondrial mobility, since
44
45 414 the ΔFgLetm1 mutation slows down the dynamic change of mitochondria
46
47 415 (Videos S1-2). Mdm38 in *S. cerevisiae* also plays a critical role in the
48
49 416 biogenesis of the respiratory chain by coupling ribosome function to protein
50
51 417 transport across the inner membrane (Frazier et al., 2006, Tamai *et al.*, 2008).
52
53
54
55
56
57
58
59
60

Proof

1 2 3 4 5 6 7 8 9 10 11 12 13 14 15 16 17 18 19 20 21 22 23 24 25 26 27 28 29 30 31 32 33 34 35 36 37 38 39 40 41 42 43 44 45 46 47 48 49 50 51 52 53 54 55 56 57 58 59 60

418 Here, we found that the protein synthesis of cytochrome *b* decreased in the
419 ΔFgLetm1 mutant (Fig. 4d). To support this idea, we conducted an affinity
420 capture assay with the FgLetm1-GFP fusion protein as a bait. Protein mass
421 spectrometry data showed that 18 proteins of the mitochondrial ribosome were
422 associated with FgLetm1 (Table S2). Among them, 12 homologous proteins
423 were also found in complex with Mdm38 and Ylh47 by affinity purification in
424 yeast (Frazier et al., 2006). Taken together, the roles of the Letm1 super-family
425 proteins in mitochondrial integrity and the biogenesis of the respiratory chain
426 seem to be highly conserved from yeast to mammals, although their amino
427 acid sequence and motif features differ among each other.

428 In addition, we also found that FgLetm1 *in F. graminearum* had some
429 distinct features from their orthologs in other organisms. For instance, Mdm38
430 is required for efficient growth on non-fermentable carbon sources, such as
431 glycerol, in yeast (Frazier et al., 2006). In contrast, the ΔFgLetm1 mutant of *F.*
432 *graminearum* showed a comparable growth phenotype on agar media
433 supplemented with either glucose or glycerol as the sole carbon source (Fig.
434 S7). Deletion of ΔFgLetm1 was strongly decreased the conidiation and septum
435 of conidia, and reduced stress response towards fungicides, ions and oxidative
436 stress. These results implied that FgLetm1 is critical for fitness in certain
437 environmental niches. Therefore, FgLetm1 may have species-specific
438 activities, in addition to the conserved function of Letm1 orthologs in
439 maintaining the integrity of mitochondria.

440 Reactive oxygen species (ROS) play a major role in pathogen-plant
441 interactions, during which the host plant rapidly triggers an oxidative burst to
442 suppress a pathogen infection. Pathogens have to cope with plant-released

Proof

1
2
3 443 ROS during a successful infection (Apel & Hirt, 2004, Heller & Tudzynski,
4
5 444 2011). Most likely, all organisms have evolved oxidative stress response (OSR)
6
7 445 mechanisms to scavenge elevated intracellular ROS levels. The ROS
8
9 446 scavenging system is important for the detoxification of ROS in the cells, and
10
11 447 the OSR has to be tightly regulated. In budding yeast, several signal
12
13 448 components are involved in the regulation of the OSR at the transcriptional
14
15 449 level, including the Hog1 cascade and the transcription factors Yap1, Atf1 and
16
17 450 Skn7 (He & Fassler, 2005, Kim & Hahn, 2013, Raitt *et al.*, 2000). In *F.*
18
19 451 *graminearum*, all three stress-related transcription factor genes, *FgAP1*,
20
21 452 *FgATF1* and *FgSKN7*, play a role in the tolerance of oxidative stress.
22
23 453 Moreover, *F. graminearum* has evolved its OSR system to transduce oxidative
24
25 454 stress as a signal for the induction of DON biosynthesis, which is a critical
26
27 455 virulence factor during the infection process (Jiang *et al.*, 2015, Montibus *et al.*,
28
29 456 2013, Van Nguyen *et al.*, 2013). A supplement of $H_2O_2$ in the cell culture of *F.*
30
31 457 *graminearum* stimulated *TRI* gene expression and increased DON
32
33 458 accumulation, in a manner largely dependent on the OSR transcription factor
34
35 459 FgSKN7 (Jiang et al., 2015). In addition to treatment of exogenous ROS,
36
37 460 endogenous ROS also modulates DON production. $H_2O_2$ was shown to
38
39 461 constitutively accumulate in the DON induction medium in the culture of *F.*
40
41 462 *graminearum.* Moreover, the time course curve of $H_2O_2$ accumulation followed
42
43 463 the pattern of DON production (Ponts et al., 2006, Ponts et al., 2007).
44
45 464 Consistence with above findings, we found that ROS was highly accumulated
46
47 465 in the mycotoxin induction medium (TBI), and exogenous $H_2O_2$ was stimulated
48
49 466 the DON production (Figs. 5, 7). We also found that deletion of *FgLETM1*
50
51 467 almost completely abolished ROS production in mitochondria in MM and TBI
52
53
54
55
56
57
58
59
60

Proof

1
2
3 468 media (Fig. 5a, Table 2), and caused the reduction of DON biosynthesis both *in*
4
5 469 *vitro* and *in planta* (Table 3). The expression of *TRI* genes and DON production
6
7 470 in ΔFgLetm1 were partially rescued in the LTB medium supplemented with
8
9 471 $H_2O_2$ (Figs. 7c-d). Therefore, the mitochondria-derived ROS was important for
10
11 472 the DON biosynthesis in *F. graminearum*, although other factors related to
12
13 473 mitochondrial dysfunction might also be involved in this process
14
15 474 (Bonnighausen *et al.*, 2015).
16
17 475 The concentration of oxygen in the atmosphere is important for the
18
19 476 biosynthesis of mycotoxins. *Penicillium griseofulvum* produced less of the
20
21 477 patulin toxin in 1% or 5% $O_2$ environment than in open air (20% $O_2$) (Paster &
22
23 478 Lisker, 1985). Ans another example, only trace amounts of T-2 toxin was
24
25 479 detected in *Fusarium sporotrichioides* under 40% $CO_2$/5% $O_2$, in comparison
26
27 480 with a much greater amount of T-2 toxin under 40% $CO_2$/20% $O_2$ (Paster *et al.*,
28
29 481 1986). Fungal growth in these gaseous environments was identical to that
30
31 482 under the open air condition, even in O2 concentrations of <1% (Hocking,
32
33 483 1989).. Here we found that *F. graminearum* showed normal growth patterns in
34
35 484 the 1% $O_2$ condition as in the open air condition (Fig. 8a), but low levels of
36
37 485 oxygen strongly reduced DON production and virulence (Fig. 8b-e), similar to
38
39 486 the phenotypes seen in the ΔFgLetm1 mutant (Figs. 6, 7). On the other hand,
40
41 487 disruption of the mitochondrial integrity in ΔFgLetm1 significantly reduced the
42
43 488 DON production (Fig. 7, table 3). We infer that fungicides targeting the
44
45 489 mitochondria might possess a potential role in controlling the DON
46
47 490 biosynthesis and FHB. We thus evaluated the effect of three mitochondrial
48
49 491 targeting fungicides including boscalid, pyraclostrobin and py-diflumetofen on
50
51 492 the DON production. As expected, all three tested fungicides strongly reduced
52
53
54
55
56
57
58
59
60

Proof

1
2
3 493 the DON production (Fig. S8). Taken together, our results suggested that
4
5 494 storage of grain under hypoxia and fungicides targeting mitochondria might
6
7 495 provide potential approaches for DON management.
8
9 496
10
11
12 497 **EXPERIMENTAL PROCEDURES**
13
14 498 **Fungal strains and culture conditions**
15
16 499 *Fusarium graminearum* strain PH-1 (NRRL 31084) was used as the progenitor
17
18 500 for constructing gene deletion mutants. The wild type and transformants
19
20 501 generated in this study were grown at 25 °C on potato dextrose agar, minimal
21
22 502 medium, and wheat-head medium for mycelial growth tests (Liu et al., 2015).
23
24 503 CMC media was used for sporulation assays (Cappelli.Ra & Peterson, 1965).
25
26 504 For quantifying the DON production, strains were grown in liquid TBI medium
27
28 505 (Menke *et al.*, 2012). To evaluate the effect of $H_2O_2$ on the induction of DON
29
30 506 biosynthesis, wild type or mutants were cultured in the LTB as described
31
32 507 (Jiang *et al.*, 2016), and $H_2O_2$ was supplemented at a final concentration of 0.5
33
34 508 mM. For hypoxia condition, the inoculated TBI or wheat heads were statically
35
36 509 incubated in a modular incubator chamber (billups-rothenberg, Inc) filled with
37
38 510 mixture gases (1% $O_2$, 99% $N_2$).
39
40 511 The sensitivity of strains towards stress agents was determined as
41
42 512 described previously (Liu et al., 2015). The final concentration of NaCl, KCl,
43
44 513 and fungicides, $Fe^{2+}$, $CaCl_2$ and $H_2O_2$ in MM were indicated in the figure. For
45
46 514 testing the temperature sensitivity of the mutants, cells were grown at 15 °C,
47
48 515 25 °C and 32 °C. The mycelial growth inhibition rate (MGIR) was calculated
49
50 516 using the formula MGIR% = [(N-C)/C]*100, where, C is colony diameter of the
51
52 517 control without treatment, and N is that with treatment. Each experiment was
53
54
55
56
57
58
59
60



Proof

1
2
3
4
5
6
7
8
9
10
11
12
13
14
15
16
17
18
19
20
21
22
23
24
25
26
27
28
29
30
31
32
33
34
35
36
37
38
39
40
41
42
43
44
45
46
47
48
49
50
51
52
53
54
55
56
57
58
59
60

518 repeated three times independently.

519 **Construction of gene deletion mutants and complemented strains**

520 Construction of gene deletion and complementation vectors and subsequent
521 transformation of *F. graminearum* were carried out using the protocols
522 described previously (Jiang *et al.*, 2011). In order to generate double mutant of
523 *FgLETM1* and *FgLETM2*, *FgLETM1* was knocked out in the *FgLETM2* deletion
524 mutant (ΔFgLETM2). The primers used to amplify the flanking sequences of
525 each gene are listed in Table S3. Deletion candidates were identified by PCR
526 with designated primers (Table S3), and were further analyzed by Southern
527 blotting. Three independent transformants for each mutant were used in all
528 experiments. FgLetm1-GFP, FgLetm2-GFP, Tri1-GFP and FgAtg8-RFP fusion
529 constructs were generated as described previously (Gu *et al.*, 2015a).

Proof

530 **Plant infection and DON production assays**

531 A 10-μl aliquot of conidial suspension ($1\times10^5$ conidia/ml) was injected into a
532 floret in the central section spikelet of single flowering wheat head of
533 susceptible cultivar grown in the field. There were ten replicates for each strain.
534 Fifteen days after inoculation, the infected spikelets in each inoculated wheat
535 head were recorded. The experiment was repeated four times, and typical
536 symptom was shown. Infectious hyphae developed in wheat tissue cells were
537 examined at 48 h post-inoculation by SEM.

538 The strain expressing the Tri1-GFP was used as the fluorescent reporter
539 strain for toxisome formation, and toxisome formation was observed after 3
540 days of incubation in TBI. The DON production in the wild type, the mutants
541 and complemented strains were quantified under several conditions, including
542 the TBI, LTB, wheat kernel medium and inoculated spikelets. The supernatant

1
2
3 543 of TBI after 7-day incubation was collected for quantification of DON. DON
4
5 544 production in wheat kernel medium was conducted as described previously
6
7 545 (Liu et al., 2015, Ji *et al.*, 2014). The inoculated spikelets were harvested after
8
9 546 fifteen days, and DON was extracted as described (Jiang et al., 2015). Total
10
11 547 amount of egrosterol was extracted from infected spikelets as described (Liu et
12
13 548 al., 2013). For ROS induction assay, LTB was used for replacement of TBI,
14
15 549 since the DON biosynthesis was already extremely induced. Recipe of LTB
16
17 550 medium was modified from TBI, only replacing the putrescine to ammonium
18
19 551 nitrate at the final concentration of 5 mM. $H_2O_2$ was daily added into the LTB to
20
21 552 the final concentration of 0.5 mM. After 7 days of incubation, the supernatant
22
23 553 was collected for DON quantification. DON samples were quantified by
24
25 554 LC-MS/MS as described previously (Dong *et al.*, 2016). The experiment was
26
27 555 repeated three times.
28
29 556 **qRT-PCR assays**
30
31 557 RNA samples of the wild type, mutants and complemented strains were
32
33 558 isolated as described (Liu et al., 2015). For the induction of *TRI* genes by $H_2O_2$,
34
35 559 the hyphae of wild type or mutant were harvested for RNA extraction after 48 h
36
37 560 of treatment. TAKARA SYBR Premix Ex Taq was used for qRT-PCR assays
38
39 561 with the CFX96 Real-Time System as described (Bio-RAD, USA). The actin
40
41 562 gene of *F. graminearum* was used as the internal control. Relative expression
42
43 563 levels of each gene were calculated with the $2^{-\Delta\Delta Ct}$ method (Livak &
44
45 564 Schmittgen, 2001).
46
47 565 **Western blotting hybridization**
48
49 566 The protein extraction and Western blot analysis were performed as described
50
51 567 previously (Yun *et al.*, 2015). Anti-MT-CYB antibody (Abcam, ab103405) was
52
53
54
55
56
57
58
59
60

Proof

1 2 3 4 5 6 7 8 9 10 11 12 13 14 15 16 17 18 19 20 21 22 23 24 25 26 27 28 29 30 31 32 33 34 35 36 37 38 39 40 41 42 43 44 45 46 47 48 49 50 51 52 53 54 55 56 57 58 59 60

568 used to detect the cytochrome b for analyzing the biosynthesis of the
569 respiratory chain. The samples were also detected with monoclonal anti-H3
570 antibody (Abcam, ab1791) as a reference. The mCherry-FgAtg8 proteolysis
571 was quantified by western blots with anti-mCherry antibody (Abcam,
572 ab167453). The samples were also detected with monoclonal anti-GAPDH
573 antibody EM1101 (Hangzhou HuaAn Biotechnology co., Ltd.) as a reference.
574 All experiments were conducted three times.

575 **Microscopy imaging**

576 Localization of green fluorescent labeled proteins and Mito-HcRed (Thermo
577 Fisher, M7512) staining signals were visualized by the Zeiss LSM780 confocal
578 microscope (Carl Zeiss AG, Germany). The microstructure of mitochondria in
579 wild type or mutants was treated as described (Yun et al., 2015) and observed
580 by the transmission electron microscope (TEM) JEOL JEM-1230. For
581 observation of infection structures on wheat glumes, the glumes were treated
582 as previous described (Gu *et al.*, 2015b), and observed in Hitachi Model
583 TM-1000 scan electron microscope (SEM) (Hitachi, Tokyo, Japan).

Proof

584 **Quantification of ATP and $H_2O_2$ production**

585 The mycelia grown in MM for 24 h and in TBI for 3 days were used for
586 quantification of $H_2O_2$ and ATP. $H_2O_2$ and ATP production were assayed using
587 the Hydrogen Peroxide Assay Kit (Beyotime Institute of Biotechnology, China,
588 S0038) and ATP Assay Kit (Beyotime, S0026), respectively. Briefly, mycelia
589 (0.05 g) were added to 200 μl of the lysis buffer in the $H_2O_2$ detection kit or 500
590 μl of the lysis buffer in the ATP detection kit. After lysis of mycelia,
591 quantification of $H_2O_2$ or ATP production was conducted following the

1
2
3 592 instructions provided by the manufacturer. Experiments were repeated three
4
5 593 times.
6
7 594
8
9
10 595 **ACKNOWLEDGEMENTS**

596 We thank Dr. Jiang Cong and Dr. Huiquan Liu (Northwest A&F University) for
597 DON quantification and bioinformatics analyses, Prof. Yunrong Chai
598 (Northeastern University, Boston) and Kevin Gozzi (Massachusetts Institute of
599 Technology) for manuscript editing. The research was supported by the
600 Natural Science Foundation of Zhejiang Province (LR17C140001), National
601 Natural Science Foundation of China (31672064), International Science &
602 Technology Cooperation Program of China (2016YFE0112900) and China
603 Agriculture Research System (CARS-3-1-15). The authors declare no conflict
604 of interest.

Proof

11 12 13 14 15 16 17 18 19 20 21 22 23 24 25 26 27 28 29 30 31 32 33 34 35 36 37 38 39 40 41 42 43 44 45 46 47 48 49 50 51 52 53 54 55 56 57 58 59 60

1
2
3 605 **REFERENCES**


606 **Apel, K. and Hirt, H.** (2004) Reactive oxygen species: Metabolism, oxidative stress,
607 and signal transduction. *Annu Rev Plant Biol,* **55,** 373-399.

608 **Audenaert, K., Callewaert, E., Hofte, M., De Saeger, S. and Haesaert, G.** (2010)
609 Hydrogen peroxide induced by the fungicide prothioconazole triggers
610 deoxynivalenol (DON) production by *Fusarium graminearum*. *BMC Microbiol,* **10**.

611 **Beckman, K. B. and Ames, B. N.** (1998) The free radical theory of aging matures.
612 *Physiol Rev,* **78,** 547-581.

613 **Bennett, J. W. and Klich, M.** (2003) Mycotoxins. *Clin Microbiol Rev,* **16,** 497-516.

614 **Boenisch, M. J., Broz, K. L., Purvine, S. O., Chrisler, W. B., Nicora, C. D.,**
615 **Connolly, L. R. Freitag, M. Baker, S. E. and Kistler, H. C.** (2017) Structural
616 reorganization of the fungal endoplasmic reticulum upon induction of mycotoxin
617 biosynthesis. *Sci Rep,* **7,** 44296.

618 **Bonnighausen, J., Gebhard, D., Kroger, C., Hadeler, B., Tumforde, T., Lieberei, R.,**
619 **Bergemann, J., Schafer, W. and Bormann, J.** (2015) Disruption of the
620 GABA shunt affects mitochondrial respiration and virulence in the cereal
621 pathogen *Fusarium graminearum*. *Mol Microbiol,* **98,** 1115-1132.

622 **Boutigny, A. L., Barreau, C., Atanasova-Penichon, V., Verdal-Bonnin, M. N.,**
623 **Pinson-Gadais, L. and Richard-Forget, F.** (2009) Ferulic acid, an efficient
624 inhibitor of type B trichothecene biosynthesis and Tri gene expression in
625 *Fusarium* liquid cultures. *Mycol Res,* **113,** 746-753.

626 **Cappelli.Ra and Peterson, J. L.** (1965) Macroconidium formation in submerged
627 cultures by a non-sporulating strain of *Gibberella Zeae*. *Mycologia,* **57,** 962-+.

628 **Desjardins, A. E.** (2006) Fusarium Mycotoxins: chemistry, genetics, and biology *APS*
629 *Press, St. Paul, Minnesota, USA*

630 **Desjardins, A. E., Hohn, T. M. and Mccormick, S. P.** (1993) Trichothecene
631 biosynthesis in *Fusarium* Species - chemistry, genetics, and significance.


Proof

*Microbiol Rev,* **57,** 595-604.

**Dimmer, K. S., Fritz, S., Fuchs, F., Messerschmitt, M., Weinbach, N., Neupert, W., *et al.*** (2002a) Genetic basis of mitochondrial function and morphology in *Saccharomyces cerevisiae*. *Mol Biol Cell,* **13,** 847-853.

**Dimmer, K. S., Fritz, S., Fuchs, F., Messerschmitt, M., Weinbach, N., Neupert, W. and Westermann, B.** (2002b) Genetic basis of mitochondrial function and morphology in Saccharomyces cerevisiae. *Mol Biol Cell,* **13,** 847-853.

**Dimmer, K. S., Navoni, F., Casarin, A., Trevisson, E., Endele, S., Winterpacht, A., Salviati, L. and Scorrano, L. (**2008) LETM1, deleted in Wolf-Hirschhorn syndrome is required for normal mitochondrial morphology and cellular viability. *Hum Mol Genet,* **17,** 201-214.

**Dong, F., Qiu, J., Xu, J., Yu, M., Wang, S., Sun, Y., Zhang, G. and Shi, J.** (2016) Effect of environmental factors on *Fusarium* population and associated trichothecenes in wheat grain grown in Jiangsu province, China. *Int J Food Microbiol,* **230,** 58-63.

**Endele, S., Fuhry, M., Pak, S. J., Zabel, B. U. and Winterpacht, A.** (1999) LETM1, a novel gene encoding a putative EF-hand $Ca^{2+}$-binding protein, flanks the Wolf-Hirschhorn syndrome (WHS) critical region and is deleted in most WHS patients. *Genomics,* **60,** 218-225.

**Frazier, A. E., Taylor, R. D., Mick, D. U., Warscheid, B., Stoepel, N., Meyer, H. E., Ryan, M. T., Guiard, B. and Rehling, P.** (2006) Mdm38 interacts with ribosomes and is a component of the mitochondrial protein export machinery. *J Cell Biol,* **172,** 553-564.

**Gardiner, D. M., Kazan, K. and Manners, J. M.** (2009) Nutrient profiling reveals potent inducers of trichothecene biosynthesis in *Fusarium graminearum*. *Fungal Genet Biol,* **46,** 604-613.

**Grissa, I., Bidard, F., Grognet, P., Grossetete, S. and Silar, P.** (2010) The

Proof

Nox/Ferric reductase/Ferric reductase-like families of Eumycetes. *Fungal Biol,* **114,** 766-777.

**Gu, Q., Chen, Y., Liu, Y., Zhang, C. and Ma, Z. H.** (2015a) The transmembrane protein FgSho1 regulates fungal development and pathogenicity via the MAPK module Ste50-Ste11-Ste7 in *Fusarium graminearum*. *New Phytol,* **206,** 315-328.

**Gu, Q., Zhang, C., Liu, X. and Ma, Z. H.** (2015b) A transcription factor FgSte12 is required for pathogenicity in *Fusarium graminearum. Mol plant pathol,* **16,** 1-13.

**Hasegawa, A. and van der Bliek, A. M.** (2007) Inverse correlation between expression of the Wolfs Hirschhorn candidate gene Letm1 and mitochondrial volume in *C. elegans* and in mammalian cells. *Hum Mol Genet,* **16,** 2061-2071.

**Hashimi, H., McDonald, L., Stribrna, E. and Lukes, J.** (2013) Trypanosome Letm1 protein Is essential for mitochondrial potassium homeostasis. *J Biol Chem,* **288,** 26914-26925.

**He, X. J. and Fassler, J. S.** (2005) Identification of novel Yap1p and Skn7p binding sites involved in the oxidative stress response of *Saccharomyces cerevisiae*. *Mol Microbiol*, **58,** 1454-1467.

**Heller, J. and Tudzynski, P.** (2011) Reactive oxygen species in phytopathogenic fungi: signaling, development, and disease. *Annu Rev Phytopathol, Vol 49,* **49,** 369-390.

**Hocking, A. D.** (1989) Responses of fungi to modified atmospheres. In: *Fumigation and Controlled Atmosphere Storage of Grain, Proceedings of an International Conference Held at Singapore.* pp. 14-18.

**Hu, S., Zhou, X. Y., Gu, X. Y., Cao, S. L., Wang, C. F. and Xu, J. R.** (2014) The cAMP-PKA pathway regulates growth, sexual and asexual differentiation, and pathogenesis in *Fusarium graminearum*. *Mol Plant Microbe In*, 27, 557-566.

**Hwang, S. K., Piao, L., Lim, H. T., Minai-Tehrani, A., Yu, K. N., Ha, Y. C., Chae, C. H., Lee, K. H., Beck, G. R., Park, J. and Cho, M. H.** (2010) Suppression of

Proof

1
2
3 686 lung tumorigenesis by Leucine Zipper/EF Hand-containing transmembrane-1.
4
5 687 *PLoS One,* **5**.
6

7 688 **Ji, F., Xu, J., Liu, X., Yin, X. and Shi, J.** (2014) Natural occurrence of deoxynivalenol
8
9 689 and zearalenone in wheat from Jiangsu province, China. *Food Chem,* **157,**
10
11 690 393-397.
12
13 691 **Jiang, C., Zhang, C., Wu, C., Sun, P., Hou, R., Liu, H. and Xu, J. R.** (2016) TRI6
14
15 692 and TRI10 play different roles in the regulation of deoxynivalenol (DON)
16
17 693 production by cAMP signalling in *Fusarium graminearum*. *Environ Microbiol,* **18,**
18
19 694 3689-3701.
20
21 695 **Jiang, C., Zhang, S. J., Zhang, Q., Tao, Y., Wang, C. F. and Xu, J. R.** (2015)
22
23 696 FgSKN7 and FgATF1 have overlapping functions in ascosporogenesis,
24
25 697 pathogenesis and stress responses in *Fusarium graminearum*. *Environ Microbiol,*
26
27 698 **17,** 1245-1260.
28
29 699 **Jiang, J., Liu, X., Yin, Y. and Ma, Z. H.** (2011) Involvement of a velvet protein FgVeA
30
31 700 in the regulation of asexual development, lipid and secondary metabolisms and
32
33 701 virulence in *Fusarium graminearum*. *PLoS One,* **6,** e28291.
34
35 702 **Jiao, F., Kawakami, A. and Nakajima, T.** (2008) Effects of different carbon sources
36
37 703 on trichothecene production and Tri gene expression by *Fusarium graminearum*
38
39 704 in liquid culture. *FEMS Microbiol Let,* **285,** 212-219.
40
41 705 **Kim, D. and Hahn, J. S.** (2013) Roles of the Yap1transcription factor and antioxidants
42
43 706 in *Saccharomyces cerevisiae*'s Ttolerance to furfural and
44
45 707 5-Hydroxymethylfurfural, which function as thiol-reactive electrophiles generating
46
47 708 oxidative stress. *Appl Environ Microbiol,* **79,** 5069-5077.
48
49
50 709 **Kimura, M., Anzai, H. and Yamaguchi, I.** (2001) Microbial toxins in plant-pathogen
51
52 710 interactions: biosynthesis, resistance mechanisms, and significance. *J Gen Appl*
53
54 711 *Microbiol,* **47,** 149-160.
55
56 712 **Kimura, M., Tokai, T., Takahashi-Ando, N., Ohsato, S. and Fujimura, M.** (2007)
57
58 713 Molecular and genetic studies of *Fusarium* trichothecene biosynthesis: Pathways,


59
60

Proof

714 genes, and evolution. *Biosci Biotech and Bioch,* **71,** 2105-2123.

715 **Liu, S. S.** (1999) Cooperation of a "reactive oxygen cycle" with the Q cycle and the
716 proton cycle in the respiratory chain - Superoxide generating and cycling
717 mechanisms in mitochondria. *J Bioenerg Biomembr,* **31,** 367-376.

718 **Liu, X., Jiang, J.H, Yin Y.N and Ma, Z. H.** (2013) Involvement of FgERG4 in
719 ergosterol biosynthesis, vegetative differentiation and virulence in *Fusarium*
720 *graminearum. Mol Plant Pathol*. **14**(1):71-83.

721 **Liu, Y., Liu, N., Yin, Y. N., Chen, Y., Jiang, J. H. and Ma, Z. H.** (2015) Histone H3K4
722 methylation regulates hyphal growth, secondary metabolism and multiple stress
723 responses in *Fusarium graminearum*. *Environ Microbiol,* **17,** 4615-4630.

724 **Livak, K. J. and Schmittgen, T. D.** (2001) Analysis of relative gene expression data
725 using real-time quantitative PCR and the $2^{-\Delta\Delta CT}$ method. *Methods,* **25,** 402-408.

726 **McQuibban, A. G., Joza, N., Megighian, A., Scorzeto, M., Zanini, D., Reipert, S.,**
727 **Richter, C., Schweyen, R. J. and Nowikovsky, K.** (2010) A *Drosophila*
728 mutant of LETM1, a candidate gene for seizures in Wolf-Hirschhorn syndrome.
729 *Hum Mol Gen,* **19,** 987-1000.

730 **Menke, J., Dong, Y. and Kistler, H. C.** (2012) *Fusarium graminearum* Tri12p
731 influences virulence to wheat and trichothecene accumulation. *Mol Plant Microbe*
732 *Interact,* **25,** 1408-1418.

733 **Mentges, M. and Bormann, J.** (2015) Real-time imaging of hydrogen peroxide
734 dynamics in vegetative and pathogenic hyphae of *Fusarium graminearum*. *Sci*
735 *Rep*, **5**, 14980.

736 **Merhej, J., Richard-Forget, F. and Barreau, C.** (2011) The pH regulatory factor Pac1
737 regulates Tri gene expression and trichothecene production in *Fusarium*
738 *graminearum*. *Fungal Genet Biol,* **48,** 275-284.

739 **Miller, J. D. and Greenhalgh, R.** (1985) Nutrient effects on the biosynthesis of
740 trichothecenes and other metabolites by *Fusarium graminearum*. *Mycologia,* **77,**

Proof

1
2
3
4
5
6
7
8
9
10
11
12
13
14
15
16
17
18
19
20
21
22
23
24
25
26
27
28
29
30
31
32
33
34
35
36
37
38
39
40
41
42
43
44
45
46
47
48
49
50
51
52
53
54
55
56
57
58
59
60

741 130-136.

742 **Missall, T. A., Lodge, J. K. and McEwen, J. E.** (2004) Mechanisms of resistance to
743 oxidative and nitrosative stress: Implications for fungal survival in mammalian
744 hosts. *Eukaryot Cell,* **3,** 835-846.

745 **Montibus, M., Ducos, C., Bonnin-Verdal, M. N., Bormann, J., Ponts, N.,**
746 **Richard-Forget, F. and Barreau, C.** (2013) The bZIP transcription factor Fgap1
747 mediates oxidative stress response and trichothecene biosynthesis but not
748 virulence in *Fusarium graminearum*. *PLoS One,* **8**.

749 **Nowikovsky, K., Froschauer, E. M., Zsurka, G., Samaj, J., Reipert, S., Kolisek, M.,**
750 **Wiesenberger, G. and Schweyen, R. J.** (2004) The LETM1/YOL027 gene
751 family encodes a factor of the mitochondrial $K^+$ homeostasis with a potential role
752 in the Wolf-Hirschhorn syndrome. *J Biol Chem,* **279,** 30307-30315.

753 **Oh, M., Son, H., Choi, G. J., Lee, C., Kim, J. C., Kim, H. and Lee Y. W.** (2016)
754 Transcription factor ART1 mediates starch hydrolysis and mycotoxin production
755 in *Fusarium graminearum* and *F. verticillioides*. *Mol Plant Pathol*, 17(5):755-768.

756 **Osiewacz, H. D.** (2002) Mitochondrial functions and aging. *Gene,* **286,** 65-71.

757 **Paster, N., Barkal G. R, and Calderon, M** (1986) Control of T-2 toxin production
758 using atmospheric gases. *J Food Protect,* **49,** 615-617.

759 **Paster, N. and Lisker, N.** (1985) Effects of controlled atmospheres on *Penicillium*
760 *patulum* growth and patulin production. *Trichothecenes and Other Mycotoxins (J.*
761 *Lacy, ed.), New York: John Wiley and Sons.*

762 **Pinson-Gadais, L., Richard-Forget, F., Frasse, P., Barreau, C., Cahagnier, B.,**
763 **Richard-Molard, D. and Bakan, B.** (2008) Magnesium represses trichothecene
764 biosynthesis and modulates *Tri5*, *Tri6*, and *Tri12* genes expression in *Fusarium*
765 *graminearum*. *Mycopathologia,* **165,** 51-59.

766 **Ponts, N., Pinson-Gadais, L., Barreau, C., Richard-Forget, F. and Ouellet, T.**
767 (2007) Exogenous $H_2O_2$ and catalase treatments interfere with Tri genes

Proof

1
2
3 768 expression in liquid cultures of *Fusarium graminearum*. *FEBS Let,* **581,** 443-447.
4
5 769 **Ponts, N., Pinson-Gadais, L., Verdal-Bonnin, M. N., Barreau, C. and**
6
7 770 **Richard-Forget, F.** (2006) Accumulation of deoxynivalenol and its 15-acetylated
8
9 771 form is significantly modulated by oxidative stress in liquid cultures of *Fusarium*
10
11 772 *graminearum*. *FEMS Microbiol Let,* **258,** 102-107.
12
13 773 **Raitt, D. C., Johnson, A. L., Erkine, A. M., Makino, K., Morgan, B., Gross, D. S.**
14
15 774 **and Johnston, L. H.** (2000) The Skn7 response regulator of *Saccharomyces*
16
17 775 *cerevisiae* interacts with Hsf1 in vivo and is required for the induction of heat
18
19 776 shock genes by oxidative stress. *Mol Bio Cell,* **11,** 2335-2347.
20
21 777 **Schlickum, S., Moghekar, A., Simpson, J. C., Steglich, C., O'Brien, R. J.,**
22
23 778 **Winterpacht, A. and Endele, S. U.** (2004) LETM1, a gene deleted in
24
25 779 Wolf-Hirschhorn syndrome, encodes an evolutionarily conserved mitochondrial
26
27 780 protein. *Genomics,* **83,** 254-261.
28
29 781 **Sickmann, A., Reinders, J., Wagner, Y., Joppich, C., Zahedi, R., Meyer, H. E.,**
30
31 782 **Schonfisch, B.., Perschil, I., Chacinska, A., Guiard, B., Rehling, P.,**
32
33 783 **Pfanner, N.and Meisinger, C.** (2003) The proteome of *Saccharomyces*
34
35 784 *cerevisiae* mitochondria. *Proc. Natl. Acad. Sci. USA,* **100,** 13207-13212.
36
37 785 **Sinha, H., David, L., Pascon, R. C., Clauder-Munster, S., Krishnakumar, S.,**
38
39 786 **Nguyen, M., Shi, G., Dean, J., Davis, R. W., Oefner, P. J., McCusker, J.**
40
41 787 **H. and Steinmetz, L. M.** (2008) Sequential elimination of major-effect
42
43 788 contributors identifies additional quantitative trait loci conditioning
44
45 789 high-temperature growth in yeast. *Genetics,* **180,** 1661-1670.
46
47 790 **Tamai, S., Iida, H., Yokota, S., Sayano, T., Kiguchiya, S., Ishihara, N.** (2008)
48
49 791 Characterization of the mitochondrial protein LETM1, which maintains the
50
51 792 mitochondrial tubular shapes and interacts with the AAA-ATPase BCS1L. *J Cell*
52
53 793 *Sci,* **121,** 2588-2600.
54
55 794 **Van Nguyen, T., Kroger, C., Bonnighausen, J., Schafer, W. and Bormann, J.**
56
57
58
59
60

Proof

(2013) The ATF/CREB transcription factor Atf1 is essential for full virulence, deoxynivalenol production, and stress tolerance in the cereal pathogen *Fusarium graminearum*. *Mol Plant-Microbe Interact,* **26,** 1378-1394.

**Wang, L., Mogg, C., Walkowiak, S., Joshi, M. and Subramaniam, R.** (2014) Characterization of NADPH oxidase genes NoxA and NoxB in *Fusarium graminearum*. *Can J Plant Pathol,* **36,** 12-21.

**Yun, Y. Z., Liu, Z. Y., Yin, Y. N., Jiang, J. H., Chen, Y., Xu, J. R. and Ma Z. H.** (2015) Functional analysis of the *Fusarium graminearum* phosphatome. *New Phytol,* **207,** 119-134.

**Zhang, B. T., Carrie, C., Ivanova, A., Narsai, R., Murcha, M. W., Duncan, O., *et al.*** (2012) LETM proteins play a role in the accumulation of mitochondrially encoded proteins in *Arabidopsis thaliana* and AtLETM2 displays parent of origin effects. *J Biol Chem,* **287,** 41757-41773.

**Zhang, C., Lin, Y., Wang, J., Wang, Y., Chen, M., Norvienyeku, J., Li, G., Yu, W. and Wang, Z. H.** (2016) FgNoxR, a regulatory subunit of NADPH oxidases, is required for female fertility and pathogenicity in *Fusarium graminearum*. *FEMS Microbiol Let,* **363,** fnv223.

**Zollino, M., Lecce, R., Fischetto, R., Murdolo, M., Faravelli, F., Selicorni, A., Butte, C., Memo, L., Capovilla, G. and Neri, G.** (2003) Mapping the Wolf-Hirschhorn syndrome phenotype outside the currently accepted WHS critical region and defining a new critical region, WHSCR-2. *Am J Hum Genet,* **72,** 590-597.

Proof

## Figure legends

**Fig. 1. Identification of the Letm1-like proteins in *Fusarium graminearum*.**

**a**. Schematic architecture of the Letm1 super-family proteins in *F. graminearum*, FgLetm1 and FgLetm2. The *Homo sapiens* Letm1 and *S. cerevisiae* Mdm38 and Ylh47 are selected as references. Conserved domains are indicated. **b**. Phylogenetic analysis of the putative Letm1-like proteins from *F. graminearum* and six plant pathogenic fungi. Amino acid sequences of the Letm1 orthologs are aligned using Clustal W and a neighbor-joining tree generated by MEGA 5.0. **c**. Transcriptional levels of the *FgLETM1* and *FgLETM2* genes in the CMC, hyphae, infected plant tissues and TBI by RNA-seq.

**Fig. 2. Phenotypes of the deletion mutants of ΔFgLetm1, ΔFgLetm2 and ΔΔFgLetm1/2 in vegetative growth, conidiogenesis and germination.**

**a**. Colony morphology of PH-1, the mutants and the complemented strains on PDA and MM at 25 °C for 3 days. **b**. Ratio of the different number of conidial septa in PH-1, mutants and complemented strains harvested from 5-day-old CMC cultures. **c**. ΔFgLetm1 reduced the conidial germination. The column labeled with star indicates a significant difference at $P = 0.05$.

**Fig. 3. ΔFgLetm1 increased the sensitivity towards osmotic stress, heat shock, fungicides and ion stresses.**

**a**. Growth phenotype of PH-1, mutants and complemented strains grown on MM without or with supplementation of NaCl or KCl after 4 days of incubation at 25 °C. **b**. Statistical analysis of the growth inhibition rate of all strains under the osmotic stresses. **c**. ΔFgLetm1 increased the sensitivity toward high temperature. Colony morphology was shown after 4 days of incubation on MM



Proof

1
2
3 842 at 15 °C and 25 °C, and 7 days of incubation at 32 °C. **d**. The transcriptional
4
5 843 level of the heat tolerant genes *FgHSP30*, *FgHSP70* and *FgGSY2* decreased
6
7 844 in the ΔFgLetm1 mutant in response to heat shock, in comparison to that in
8
9 845 PH-1. The expression levels of each gene at 25 °C for 16 h were set to 1. **e**.
10
11 846 The ΔFgLetm1 mutant was more sensitive towards fungicides iprodione,
12
13 847 phenamacril, and ion stresses than that of the wild type. Plates were incubated
14
15 848 at 25 °C for 4 days before imaging. **f**. Statistical analysis of the growth
16
17 849 inhibition rate of strains towards above stresses. Values on the bars followed
18
19 850 by the same letter mean no significant difference at $P = 0.05$.
20
21 851 **Fig. 4. FgLetm1 is localized to mitochondria and critical for the**
22
23 852 **mitochondrial integrity.**
24
25 853 **a**. Both FgLetm1 and FgLetm2 are localized to the mitochondria. Mycelia of
26
27 854 FgLetm1-C and FgLetm2-C were grown in CM and stained with Mito-HcRed.
28
29 855 Images were taken by confocal fluorescent microscope. Bar=10 μm. b.
30
31 856 ΔFgLetm1 changed the mitochondrial structural patterns. Strains were grown
32
33 857 in CM broth for 16 h at 25 °C, then harvested and stained with Mito-HcRed for
34
35 858 observation. Typical patterns in individual strain were shown. Bar= 10 μm. **c**.
36
37 859 ΔFgLetm1 mutant caused mitochondrial swelling. Ultrastructural morphology
38
39 860 of mitochondria in each strain was visualized by transmission electron
40
41 861 microscope. Bars were indicated in images. **d**. ΔFgLetm1 decreased the
42
43 862 protein level of cytochrome *b* (Cyt *b*), an indicator protein of respiratory chain
44
45 863 components. The protein abundance of Cyt *b* in the PH-1 and mutants were
46
47 864 analyzed by immunoblot assays. The histone H3 was used as a reference
48
49 865 protein.
50
51 866 **Fig. 5. Deletion mutant of ΔFgLetm1 decreased the concentration of**
52
53
54
55
56
57
58
59
60

Proof

1 2 3 4 5 6 7 8 9 10 11 12 13 14 15 16 17 18 19 20 21 22 23 24 25 26 27 28 29 30 31 32 33 34 35 36 37 38 39 40 41 42 43 44 45 46 47 48 49 50 51 52 53 54 55 56 57 58 59 60

867 **endogenous reactive oxygen species (ROS).**

868 **a**. ΔFgLetm1 strongly reduced the endogenous ROS in MM and TBI. Hyphae
869 grown in MM for 24 h, or TBI for 3 days were stained by the ROS indicator,
870 H2DCFDA. Bar=10 μm. **b**. Mutant of ΔFgLetm1 and ΔΔFgLetm1/2 decreased
871 the transcriptional level of genes encoding catalases and superoxide
872 dismutases in TBI. **c**. Mutant of ΔFgLetm1 and ΔΔFgLetm1/2 increased the
873 resistance towards the oxidative stress by $H_2O_2$. Strains were grown on MM
874 with or without 10 mM $H_2O_2$ for 4 days at 25°C. **d**. Statistical analysis of the
875 growth inhibition rate of PH-1, mutants and complemented strains towards the
876 oxidative stress generated by $H_2O_2$. Values on the bars followed by the same
877 letter indicate no significant difference at $P = 0.01$.

878 **Fig. 6 Deletion mutants of ΔFgLetm1 and ΔΔFgLetm1/2 were attenuated**
879 **in virulence *in planta*.**

880 **a**. Dissection of infected wheat heads caused by PH-1, the mutants and the
881 complemented strains. Inoculated ears were dissected at 15 dpi. Inoculated
882 sites were indicated with red arrows. **b**. Infection structures on glumes infected
883 by PH-1, mutants and complemented strains. The inoculated glumes were
884 collected after 2 dpi with conidia, and observed by SEM. The infection
885 structures were pointed out by red arrows, and details were enlarged.

886 **Fig. 7. Deletion mutants of ΔFgLetm1 and ΔΔFgLetm1/2 reduced the DON**
887 **biosynthesis *in vitro* and *in planta*.**

888 **a**. ΔFgLetm1 significantly decreased the transcriptional level of *TRI* genes in
889 TBI medium. **b**. Toxisome formation of PH-1, ΔFgLetm1 and ΔFgLetm2.
890 Strains were labeled with Tri1-GFP and incubated in TBI for 3 days, and
891 toxisomes were observed by confocal fluorescent microscope. Bar=10 μm. **c**.

Proof

1
2
3 892 Induction of DON biosynthesis by $H_2O_2$ in wild type and ΔFgLetm1 grown in
4
5 893 LTB medium. $H_2O_2$ was added into LTB daily, and the supernatant after 7 days
6
7 894 of incubation was used for the quantification of DON production. **d**. Relative
8
9 895 expression levels of *TRI5*, *TRI6* and *TRI10* in PH-1 and ΔFgLetm1 with or
10
11 896 without $H_2O_2$ treatment. The relative expression level of each gene in wild type
12
13 897 without $H_2O_2$ treatment was arbitrarily set to 1. Values on the bars followed by
14
15 898 the same letter indicate no significant difference at $P$ = 0.05.
16
17 899 **Fig. 8. DON biosynthesis and virulence were reduced under hypoxia**
18
19 900 **conditions.**
20
21 901 **a**. Colony morphology of wild type grown on PDA in the open air and hypoxia
22
23 902 conditions. **b**. Relative expression level of *TRI5*, *TRI6* and *TRI10* in the
24
25 903 mycelium of PH-1 under open air and hypoxia conditions. Strains were grown
26
27 904 in TBI for 3 days. The pigment biosynthesis gene, *AURJ*, was used as a
28
29 905 control. **c**. Toxisome formation of the wild type under open air and hypoxia
30
31 906 conditions. The Tri1-GFP was observed after 3 days of incubation. **d**. DON
32
33 907 production of wild type under open air and hypoxia conditions after 7 days of
34
35 908 incubation. **e**. Virulence of wild type under open air and hypoxia conditions.
36
37 909 Scab symptom was taken after 7 dpi.
38
39
40
41
42
43
44
45
46
47
48
49
50
51
52
53
54
55
56
57
58
59
60

Proof

1
2
3 910 **Supplemental figure, table and video legends**

911 **Fig. S1. Phylogenetic tree of the Letm1 super-family orthologs from 32 fungal genomes available in the NCBI Bioprojects and Broad Institute databases.** Orthologs were retrieved with the yeast Letm1 proteins, Mdm38 and Ylh47, and FgLetm1 and FgLetm2 protein sequences as queries. The phylogenetic tree was constructed by the neighbor-joining method using MEGA 5.0. Numbers at the node represent the results of 1000 bootstrap replications. The GenBank or organism-specific accession numbers are indicated in the figure.

919 **Fig. S2. Identification of deletion mutants and complemented strains.** **a**. Southern blot hybridization analysis of the deletion mutant of ΔFgLetm1, ΔΔFgLetm1/2, and the complemented strain ΔFgLetm1+$P_{LETM1}$ FgLetm1-GFP using downstream DNA fragments of *FgLETM1* as the probe. Both ΔFgLetm1 and ΔΔFgLetm1/2 had an anticipated 4594 bp band, but both of them lacked the 2219 bp band present in wild-type PH-1, when probed with a 725 bp downstream DNA fragment of *FgLETM1*. **b**. Southern blot hybridization analysis of the deletion mutant of ΔFgLetm2, ΔΔFgLetm1/2, and the complemented strain ΔFgLetm2+$P_{LETM2}$ FgLetm2-GFP using a downstream DNA fragment of *FgLETM2* as the probe. Using an 800 bp upstream DNA fragment of *FgLETM2* as the probe, ΔFgLetm2 mutant had an anticipated 3253 bp band, when the chromosomal DNA of ΔFgLetm2 was digested with *NdeI*. ΔΔFgLetm1/2 presented a 4098 bp band but lacked the 1585 bp band present in the wild-type PH-1, when the chromosomal DNA of ΔΔFgLetm1/2 was digested with *EcoRV* and blotted with the same probe. **c**. PCR verification of complemented strain ΔFgLetm1+$P_{LETM1}$ FgLetm1-GFP, and

Proof

1
2
3 935 ΔFgLetm2+P$_{LETM2}$ FgLetm2-GFP. The whole cassette including the promoter,
4
5 936 ORF and gfp was amplified, respectively.
6
7 937 **Fig. S3. Conidial morphology of the wild type, ΔFgLetm1, ΔFgLetm2,**
8
9
10 938 **ΔΔFgLetm1/2 and the complemented strains. T**he septa were stained with
11
12 939 calcofluor white and observed by fluorescent microscope. Bar= 20 μm.
13
14 940 **Fig. S4. Colony morphology of PH-1, the mutants and the complemented**
15
16 941 **strains on wheat head medium (WA) at 25 °C for 3 days.**
17
18 942 **Fig. S5. Infection structure of wild type and deletion mutant of ΔFgLetm1**
19
20
21 943 **on the inoculated glumes at 14 days post-inoculation.** Samples were
22
23 944 collected after 2 weeks post-inoculation and observed by the scan electron
24
25 945 microscope. Bars were indicated on the images.
26
27 946 **Fig. S6. Induction of DON biosynthesis by exogenous ATP in the wild**
28
29
30 947 **type and mutants grown in TBI medium.** ATP was added into TBI with at the
31
32 948 final concentration of 10 μM, and the cell free supernatant after 7 days of
33
34 949 incubation was used for the quantification of DON production. Error bars
35
36 950 denote standard deviation from three repeated experiments.
37
38 951 **Fig. S7. Deletion mutant of ΔFgLetm1 was not changed the utilization of**
39
40
41 952 **non-fermentable carbon.** Colony morphology of the wild type, ΔFgLetm1,
42
43 953 ΔFgLetm2 and ΔΔFgLetm1/2 on minimal medium supplemented with glucose
44
45
46 954 or glycerol as a sole carbon source. Plates were photographed after incubation
47
48 955 at 25 °C for 3 days.
49
50 956 **Fig. S8. Fungicides targeting mitochondria are able to inhibit the**
51
52 957 **toxisome formation and DON biosynthesis.**
53
54 958 **a**. The growth inhibition of tested fungicides at 0.3 μg/ml. **b**. Toxisome
55
56 959 formation of fungicides at 0.3 μg/ml. The ΔTri1:Tri1-GFP strain was grown in
57
58
59
60

Proof

1
2
3 960 TBI for 24 h, then individual fungicide was added at the final concentration at
4
5 961 0.3 μg/ml and incubated for another 24 h before observation. **c**. The DON
6
7 962 production of each treatment. The DON was extracted from the 7-day cultured
8
9 963 TBI in each treatment and quantified by LC-MS. Column followed by different
10
11 964 letter indicated a significantly difference at $P = 0.05$.
12
13 965 **Table S1** The Letm1-superfamily domain in the Letm1 orthologues of 6
14
15 966 filamentous plant pathogenic fungi and *Saccharomyces cerevisiae*.
16
17 967 **Table S2** Proteins of the mitochondrial ribosome in complex with FgLetm1 by
18
19 968 affinity purification and mass spectrometry assay.
20
21 969 **Table S3**. Oligonucleotide primers used in this study.
22
23 970 **Video 1.** Mitochondrial patterns stained by Mito-HcRed in the wild type.
24
25 971 **Video 2.** Mitochondrial patterns stained by Mito-HcRed in deletion mutant of
26
27 972 ΔFgLetm1.
28
29
30
31
32
33
34
35
36
37
38
39
40
41
42
43
44
45
46
47
48
49
50
51
52
53
54
55
56
57
58
59
60

Proof

1
2
3
4
5
6
7
8
9
10
11
12
13
14
15
16
17
18
19
20
21
22
23
24
25
26
27
28
29
30
31
32
33
34
35
36
37
38
39
40
41
42
43
44
45
46
47
48
49
50
51
52
53
54
55
56
57
58
59
60

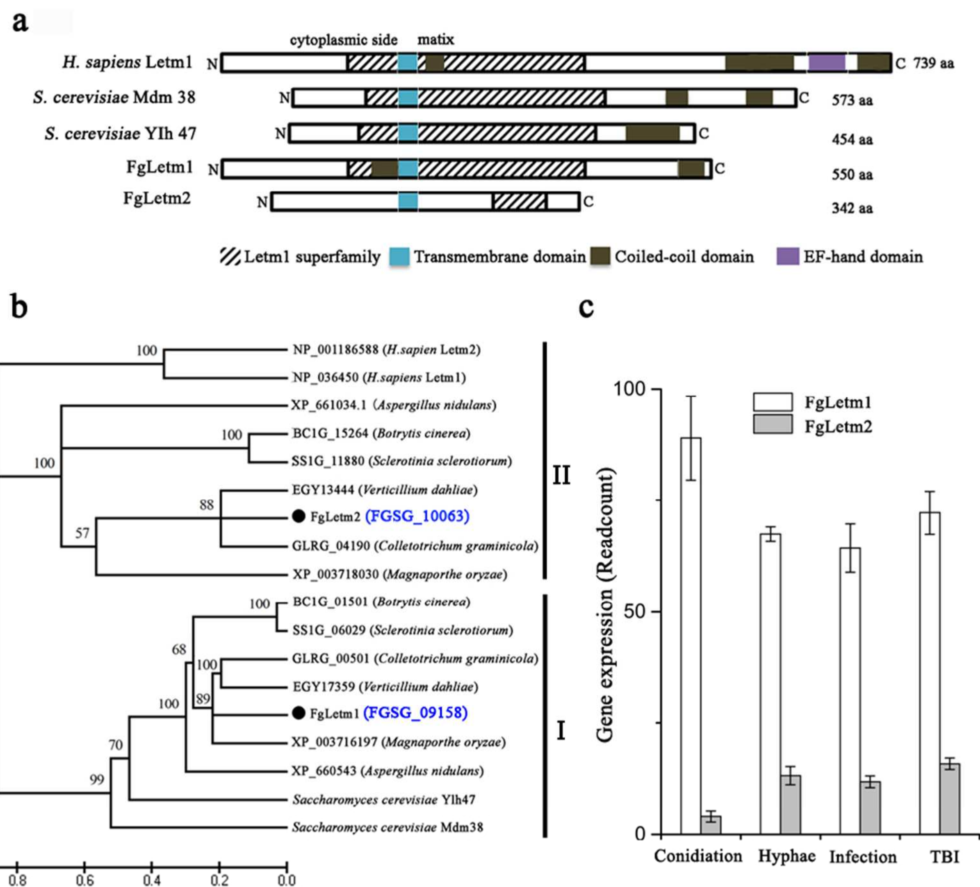


Fig. 1. Identification of the Letm1-like proteins in Fusarium graminearum. a. Schematic architecture of the Letm1 super-family proteins in F. graminearum, FgLetm1 and FgLetm2. The Homo sapiens Letm1 and S. cerevisiae Mdm38 and Ylh47 are selected as references. Conserved domains are indicated. b. Phylogenetic analysis of the putative Letm1-like proteins from F. graminearum and six plant pathogenic fungi. Amino acid sequences of the Letm1 orthologs are aligned using Clustal W and a neighbor-joining tree generated by MEGA 5.0. c. Transcriptional levels of the FgLETM1 and FgLETM2 genes in the CMC, hyphae, infected plant tissues and TBI by RNA-seq.

80x73mm (300 x 300 DPI)

1
2
3
4
5
6
7
8
9
10
11
12
13
14
15
16
17
18
19
20
21
22
23
24
25
26
27
28
29
30
31
32
33
34
35
36
37
38
39
40
41
42
43
44
45
46
47
48
49
50
51
52
53
54
55
56
57
58
59
60

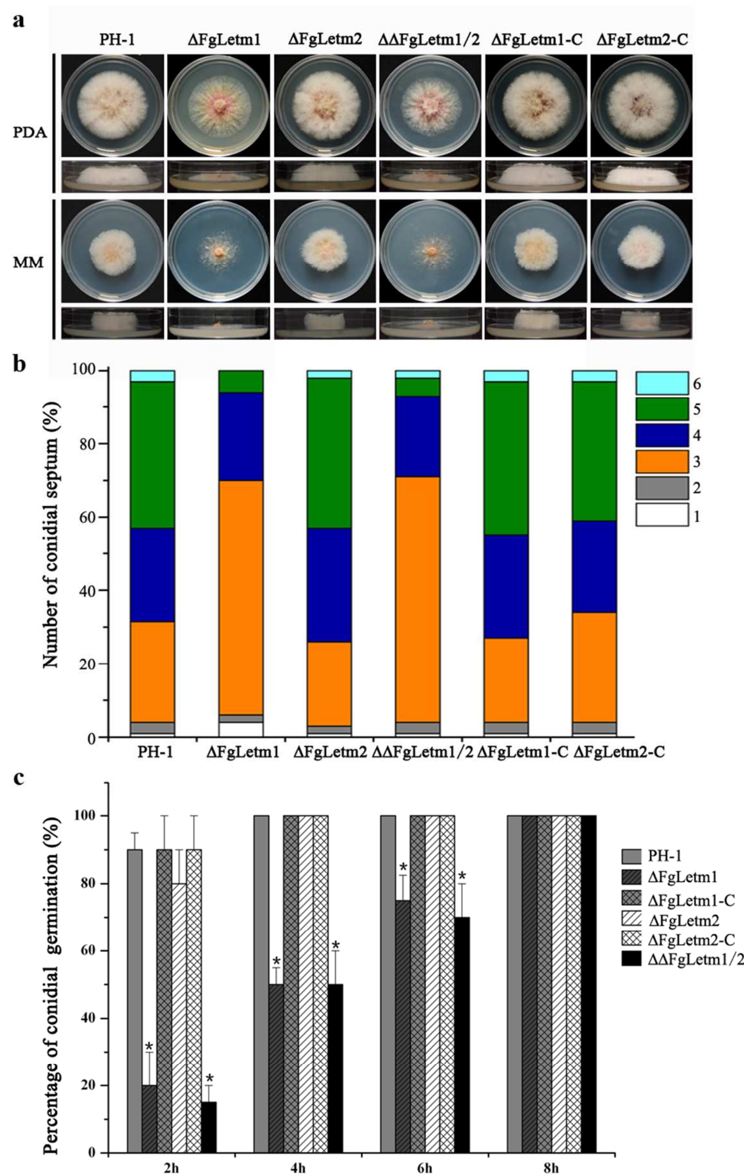


Fig. 2. Phenotypes of the deletion mutants of ΔFgLetm1, ΔFgLetm2 and ΔΔFgLetm1/2 in vegetative growth, conidiogenesis and germination.
a. Colony morphology of PH-1, the mutants and the complemented strains on PDA and MM at 25 °C for 3 days. b. Ratio of the different number of conidial septa in PH-1, mutants and complemented strains harvested from 5-day-old CMC cultures. c.ΔFgLetm1 reduced the conidial germination. The column labeled with star indicates a significant difference at P = 0.05.

80x128mm (300 x 300 DPI)

1
2
3
4
5
6
7
8
9
10
11
12
13
14
15
16
17
18
19
20
21
22
23
24
25
26
27
28
29
30
31
32
33
34
35
36
37
38
39
40
41
42
43
44
45

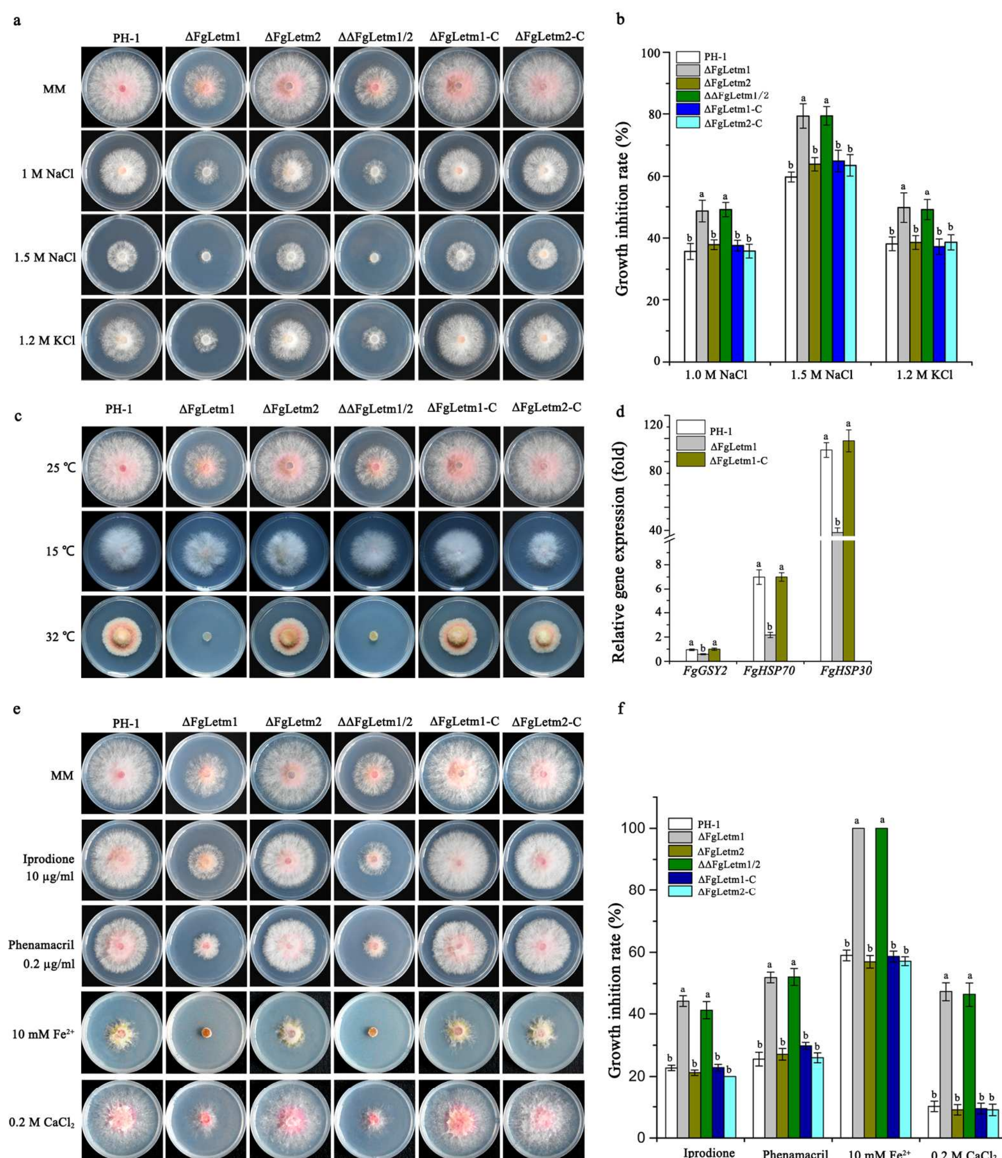


46
47
48
49
50
51
52
53
54
55
56

Fig. 3. ΔFgLetm1 increased the sensitivity towards osmotic stress, heat shock, fungicides and ion stresses. a. Growth phenotype of PH-1, mutants and complemented strains grown on MM without or with supplementation of NaCl or KCl after 4 days of incubation at 25 °C. b. Statistical analysis of the growth inhibition rate of all strains under the osmotic stresses. c. ΔFgLetm1 increased the sensitivity toward high temperature. Colony morphology was shown after 4 days of incubation on MM at 15 °C and 25 °C, and 7 days of incubation at 32 °C. d. The transcriptional level of the heat tolerant genes FgHSP30, FgHSP70 and FgGSY2 decreased in the ΔFgLetm1 mutant in response to heat shock, in comparison to that in PH-1. The expression levels of each gene at 25 °C for 16 h were set to 1. e. The ΔFgLetm1 mutant was more sensitive towards fungicides iprodione, phenamacril, and ion stresses than that of the wild type. Plates were incubated at 25 °C for 4 days before imaging. f. Statistical analysis of the growth inhibition rate of strains towards above stresses. Values on the bars followed by the same letter mean no significant difference at P = 0.05.

57
58
59
60

1
2
3 170x202mm (300 x 300 DPI)
4
5
6
7
8
9
10
11
12
13
14
15
16
17
18
19
20
21
22
23
24
25
26
27
28
29
30
31
32
33
34
35
36
37
38
39
40
41
42
43
44
45
46
47
48
49
50
51
52
53
54
55
56
57
58
59
60

Proof

1
2
3
4
5
6
7
8
9
10
11
12
13
14
15
16
17
18
19
20
21
22
23
24
25
26
27
28
29
30
31
32
33
34
35
36
37
38
39
40
41
42
43
44
45
46
47
48
49
50
51
52
53
54
55
56
57
58
59
60

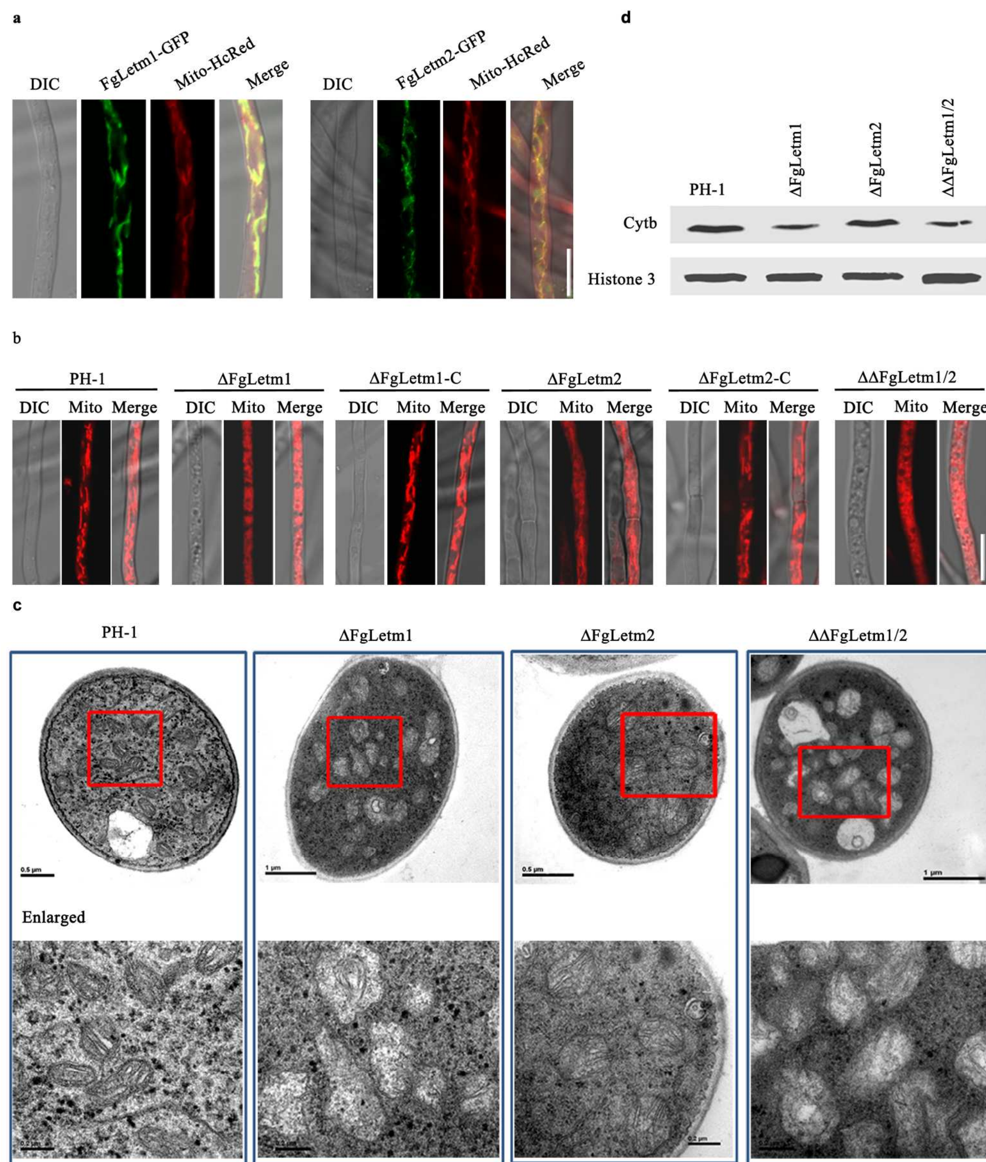


Fig. 4. FgLetm1 is localized to mitochondria and critical for the mitochondrial integrity.
a. Both FgLetm1 and FgLetm2 are localized to the mitochondria. Mycelia of FgLetm1-C and FgLetm2-C were grown in CM and stained with Mito-HcRed. Images were taken by confocal fluorescent microscope. Bar=10 μm. b. ΔFgLetm1 changed the mitochondrial structural patterns. Strains were grown in CM broth for 16 h at 25 °C, then harvested and stained with Mito-HcRed for observation. Typical patterns in individual strain were shown. Bar= 10 μm. c. ΔFgLetm1 mutant caused mitochondrial swelling. Ultrastructural morphology of mitochondria in each strain was visualized by transmission electron microscope. Bars were indicated in images. d. ΔFgLetm1 decreased the protein level of cytochrome b (Cyt b), an indicator protein of respiratory chain components. The protein abundance of Cyt b in the PH-1 and mutants were analyzed by immunoblot assays. The histone H3 was used as a reference protein.

170x200mm (300 x 300 DPI)

1
2
3
4
5
6
7
8
9
10
11
12
13
14
15
16
17
18
19
20
21
22
23
24
25
26
27
28
29
30
31
32
33
34
35
36
37
38
39
40
41
42
43
44
45
46
47
48
49
50
51
52
53
54
55
56
57
58
59
60

Proof

1
2
3
4
5
6
7
8
9
10
11
12
13
14
15
16
17
18
19
20
21
22
23
24
25
26
27
28
29
30
31
32
33
34
35
36
37
38
39
40
41
42
43
44
45
46
47
48
49
50
51
52
53
54
55
56
57
58
59
60

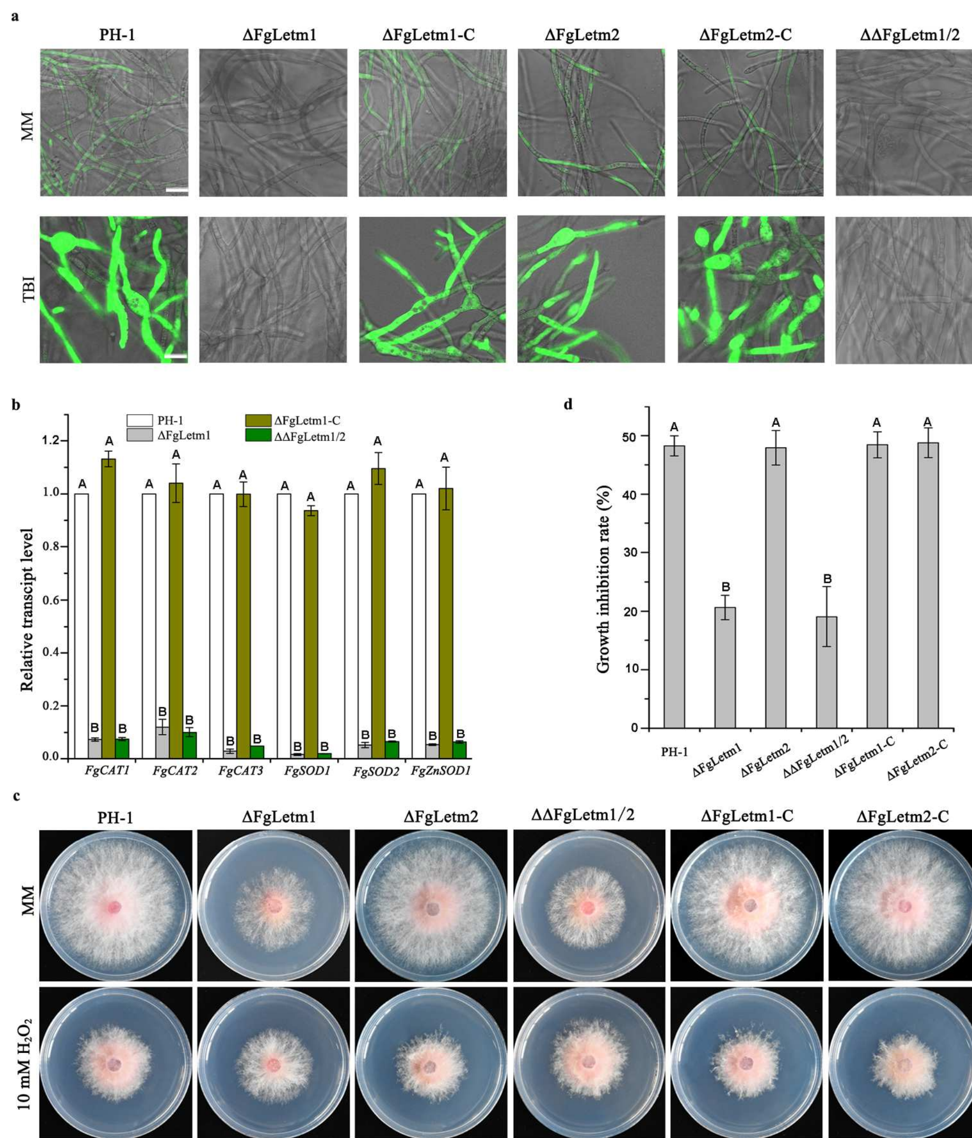


Fig. 5. Deletion mutant of ΔFgLetm1 decreased the concentration of endogenous reactive oxygen species (ROS).

a. ΔFgLetm1 strongly reduced the endogenous ROS in MM and TBI. Hyphae grown in MM for 24 h, or TBI for 3 days were stained by the ROS indicator, H2DCFDA. Bar=10 μm. b. Mutant of ΔFgLetm1 and ΔΔFgLetm1/2 decreased the transcriptional level of genes encoding catalases and superoxide dismutases in TBI. c. Mutant of ΔFgLetm1 and ΔΔFgLetm1/2 increased the resistance towards the oxidative stress by H2O2. Strains were grown on MM with or without 10 mM H2O2 for 4 days at 25°C. d. Statistical analysis of the growth inhibition rate of PH-1, mutants and complemented strains towards the oxidative stress generated by H2O2. Values on the bars followed by the same letter indicate no significant difference at P = 0.01.

170x198mm (300 x 300 DPI)

1
2
3
4
5
6
7
8
9
10
11
12
13
14
15
16
17
18
19
20
21
22
23
24
25
26
27
28
29
30
31
32
33
34
35
36
37
38
39
40
41
42
43
44
45
46
47
48
49
50
51
52
53
54
55
56
57
58
59
60

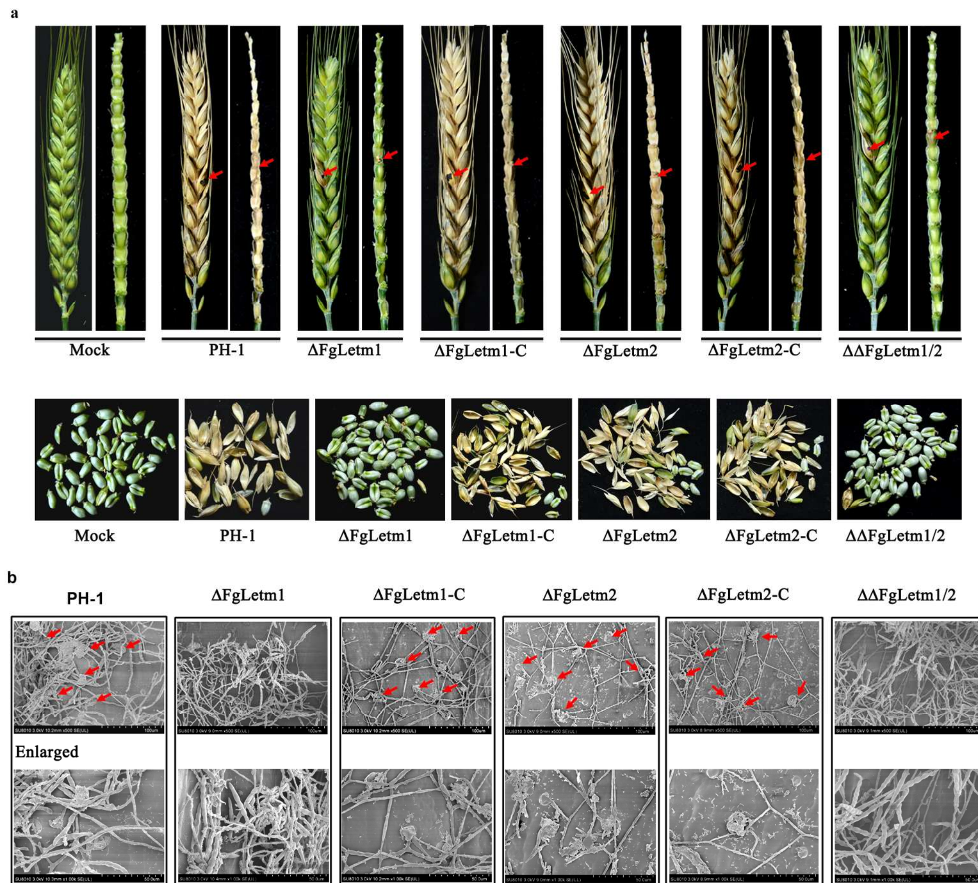


Fig. 6 Deletion mutants of ΔFgLetm1 and ΔΔFgLetm1/2 were attenuated in virulence in planta. a. Dissection of infected wheat heads caused by PH-1, the mutants and the complemented strains. Inoculated ears were dissected at 15 dpi. Inoculated sites were indicated with red arrows. b. Infection structures on glumes infected by PH-1, mutants and complemented strains. The inoculated glumes were collected after 2 dpi with conidia, and observed by SEM. The infection structures were pointed out by red arrows, and details were enlarged.

170x157mm (300 x 300 DPI)

1
2
3
4
5
6
7
8
9
10
11
12
13
14
15
16
17
18
19
20
21
22
23
24
25
26
27
28
29
30
31
32
33
34
35
36
37
38
39
40
41
42
43
44
45
46
47
48
49
50
51
52
53
54
55
56
57
58
59
60

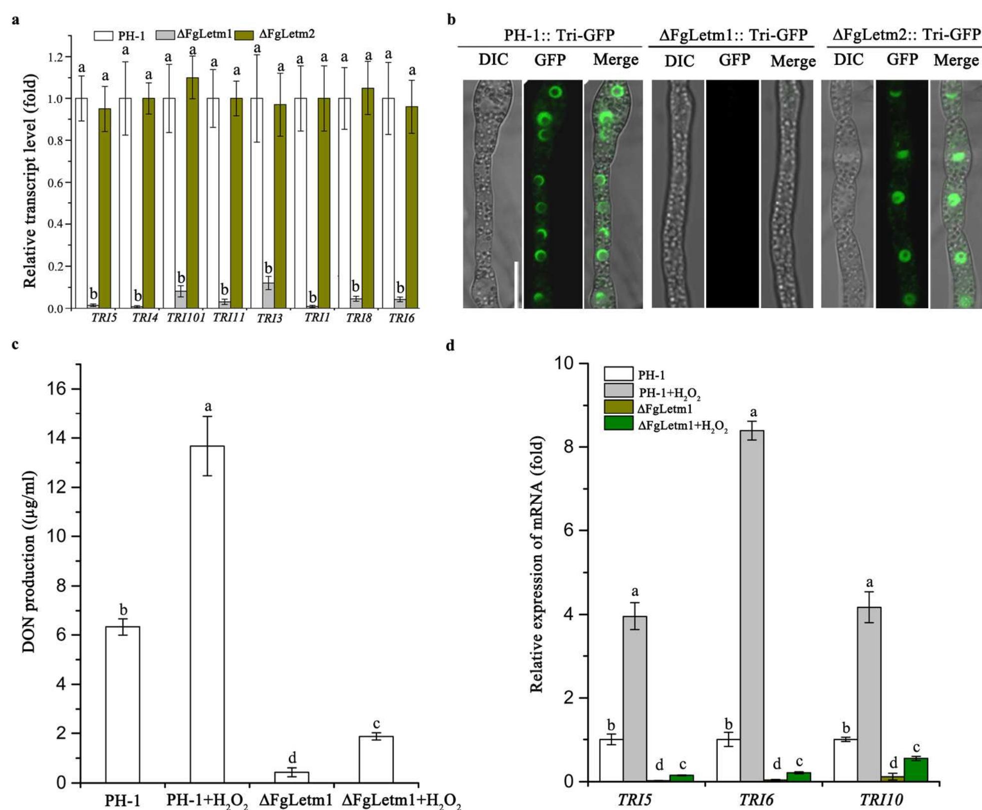


Fig. 7. Deletion mutants of ΔFgLetm1 and ΔΔFgLetm1/2 reduced the DON biosynthesis in vitro and in planta.
a. ΔFgLetm1 significantly decreased the transcriptional level of TRI genes in TBI medium. b. Toxisome formation of PH-1, ΔFgLetm1 and ΔFgLetm2. Strains were labeled with Tri1-GFP and incubated in TBI for 3 days, and toxisomes were observed by confocal fluorescent microscope. Bar=10 μm. c. Induction of DON biosynthesis by H2O2 in wild type and ΔFgLetm1 grown in LTB medium. H2O2 was added into LTB daily, and the supernatant after 7 days of incubation was used for the quantification of DON production. d. Relative expression levels of TRI5, TRI6 and TRI10 in PH-1 and ΔFgLetm1 with or without H2O2 treatment. The relative expression level of each gene in wild type without H2O2 treatment was arbitrarily set to 1. Values on the bars followed by the same letter indicate no significant difference at P = 0.05.

170x143mm (300 x 300 DPI)

1
2
3
4
5
6
7
8
9
10
11
12
13
14
15
16
17
18
19
20
21
22
23
24
25
26
27
28
29
30
31
32
33
34
35
36
37
38
39
40
41
42
43
44
45
46
47
48
49
50
51
52
53
54
55
56
57
58
59
60

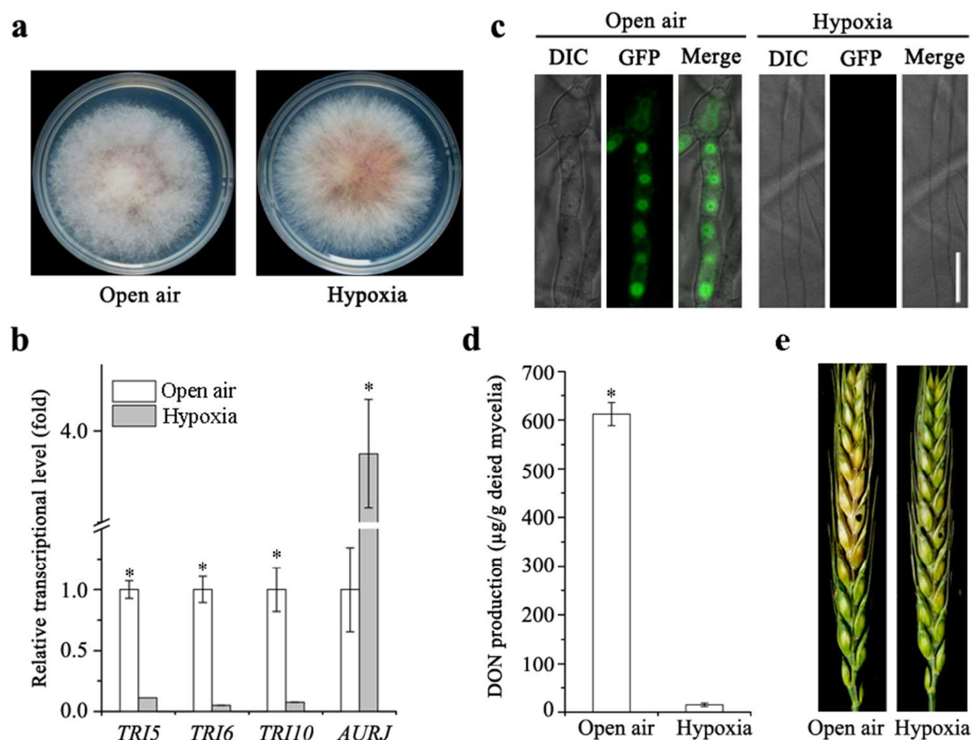


Fig. 8. DON biosynthesis and virulence were reduced under hypoxia conditions.
a. Colony morphology of wild type grown on PDA in the open air and hypoxia conditions. b. Relative expression level of TRI5, TRI6 and TRI10 in the mycelium of PH-1 under open air and hypoxia conditions. Strains were grown in TBI for 3 days. The pigment biosynthesis gene, AURJ, was used as a control. c. Toxisome formation of the wild type under open air and hypoxia conditions. The Tri1-GFP was observed after 3 days of incubation. d. DON production of wild type under open air and hypoxia conditions after 7 days of incubation. e. Virulence of wild type under open air and hypoxia conditions. Scab symptom was taken after 7 dpi.

80x62mm (300 x 300 DPI)

1 2 3 4 5 6 7 8 9 10 11 12 13 14 15 16 17 18 19 20 21 22 23 24 25 26 27 28 29 30 31 32 33 34 35 36 37 38 39 40 41 42 43 44 45 46 47 48 49 50 51 52 53 54 55 56 57 58 59 60

1 **Table 1 Vegetative growth and conidiation of *Fusarium graminearum***
2 **strains**

| Strain | Growth rate (cm/day) | Conidiation Production ($\times 10^5$) | Conidial length (μm) |
|---|---|---|---|
| PH-1 | 2.43±0.06[a*] | 6.15±0.47[a] | 63.50±6.10[a] |
| ΔFgLetm1 | 2.06±0.03[b] | 4.65±0.53[b] | 38.88±4.39[b] |
| Δ FgLetm1-C | 2.40±0.04[a] | 6.28±0.48[a] | 63.13±8.04[a] |
| Δ FgLetm2 | 2.32±0.02[a] | 6.03±0.38[a] | 56.50±5.07[a] |
| Δ FgLetm2-C | 2.37±0.02[a] | 5.98±0.26[a] | 59.88±2.10[a] |
| Δ FgLetm12 | 2.03±0.03[b] | 5.20±0.34[b] | 41.25±3.57[b] |

3

4 [*]Values followed by the same letter are not significantly different at $P$ = 0.05 for each
5 treatment.

Proof

1
2
3
4
5
6
7 1 **Table 2 Productions of ATP, hydrogen peroxide and ethanol in PH-1, mutants and complemented strains**
8 2

| Strain | ATP (μM) | | $H_2O_2$ (mM) | | Ethanol (mg/ml) |
|---|---|---|---|---|---|
| | MM | TBI | MM | TBI | MM |
| PH-1 | 1341.35±29.24[a*] | 1360.05±42.46 [a] | 24.97±2.14 [a] | 133.94±9.85 [a] | 2.16±0.07 [b] |
| ΔFgLetm1 | 1008.54±34.32[b] | 902.17±23.46 [b] | 3.26±0.18 [b] | 4.51±0.36 [b] | 4.32±0.12 [a] |
| Δ FgLetm1-C | 1320.14±13.11 [a] | 1358.23±35.23 [a] | 20.67±3.25 [a] | 120.55±20.11 [a] | 2.3±0.21 [b] |
| Δ FgLetm2 | 1300.02±24.53 [a] | 1250.22±48.37 [a] | 19.66±1.67 [b] | 122.63±15.37 [a] | 2.43±0.20 [b] |
| Δ FgLetm2-C | 1360.56±15.21 [a] | 1400.26±68.70 [a] | 21.79±3.22 [a] | 120.33±18.54 [a] | 2.1±0.25 [b] |
| Δ FgLetm12 | 953.56±30.14 [b] | 875.65±50.32 [b] | 2.34±0.86 [b] | 2.56±0.25 [b] | 4.17±0.14 [a] |

3
4 [*]Values followed by the same letter are not significantly different at $P = 0.05$ for each treatment.

Proof

20
21
22
23
24
25
26
27
28
29
30
31
32
33
34
35
36
37
38
39
40
41
42
43
44
45
46
47
48
49

**Table 3 Deoxynivalenol productions of the wild type, mutants and complemented strains in TBI, wheat kernel medium and infected spikelets**

| | TBI | Wheat kernel | Infected spikelet |
|---|---|---|---|
| Strain | DON production (μg/g dried mycelia) | DON production (μg/mg ergosterol) | DON production (mg/mg ergosterol) |
| PH-1 | 650.75±7.07[a*] | 398.88±13.07[a] | 581.53±30.28[a] |
| ΔFgLetm1 | 38.24±2.81[b] | 11.81±1.40[b] | 228.61±20.25[b] |
| Δ FgLetm1-C | 630.80±12.86[a] | 428.56±14.59[a] | 536.27±17.36[a] |
| Δ FgLetm2 | 635.07±13.80[a] | 420.97±15.58[a] | 566.54±30.85[a] |
| Δ FgLetm2-C | 660.46±8.96[a] | 394.22±15.08[a] | 605.03±35.18[a] |
| Δ FgLetm12 | 35.93±3.53[b] | 9.43±2.89[b] | 188.10±19.51[b] |

[*]Values followed by the same letter are not significantly different at $P$ = 0.05 for each treatment.

Proof